Fatty Acid Preservation in Modern and Relict Hot-Spring Deposits in Iceland, with Implications for Organics Detection on Mars

Amy Williams, Kathleen Craft, Maëva Millan, Sarah Stewart Johnson, Christine Knudson, Marisol Juarez Rivera, Amy Mcadam, Dominique Tobler, John Roma Skok

Astrobiology

Astrobiology Manuscript Central: http://mc.manuscriptcentral.com/astrobiology

Fatty Acid Preservation in Modern and Relict Hot Spring Deposits in Iceland, with Implications for Organics Detection on Mars

Journal:	*Astrobiology*
Manuscript ID	AST-2019-2115.R3
Manuscript Type:	Special Collection: Hot Springs Van Kronendonk Ed
Date Submitted by the Author:	n/a
Complete List of Authors:	Williams, Amy; University of Florida, Department of Geological Sciences; NASA Goddard Space Flight Center, Planetary Environments Laboratory Craft, Kathleen; Johns Hopkins University Applied Physics Laboratory Millan, Maeva; Georgetown University, Department of Biology; NASA Goddard Space Flight Center, Planetary Environments Laboratory Johnson, Sarah; Georgetown University, Department of Biology; Georgetown University, Science, Technology, and International Affairs Program Knudson, Christine; NASA Goddard Space Flight Center, Planetary Environments Laboratory; University of Maryland at College Park College of Computer Mathematical and Natural Sciences, Center for Research and Exploration in Space Science and Technology Juarez Rivera, Marisol; Arizona State University McAdam, Amy; NASA Goddard Space Flight Center, Planetary Environments Laboratory Tobler, Dominique; University of Copenhagen, Department of Chemistry Skok, J.R.; SETI Institute
Keyword:	Hot Springs, Organic Geochemistry, Mars, Analog, Biosignatures
Manuscript Keywords (Search Terms):	hot springs, sinter, FAME, MSL, Sample Analysis at Mars (SAM) instrument, TMAH

Fatty Acid Preservation in Modern and Relict Hot Spring Deposits in Iceland, with Implications for Organics Detection on Mars

Running Title: Organics Preservation in Icelandic Hot Springs

Amy J. Williams[1,2*], Kathleen L. Craft[3], Maëva Millan[2,4], Sarah Stewart Johnson[4,5], Christine A. Knudson[2,6], Marisol Juarez Rivera[7], Amy C. McAdam[2], Dominique Tobler[8], J.R. Skok[9]

[1] Department of Geological Sciences, University of Florida, Gainesville, FL, USA

[2] Planetary Environments Laboratory (Code 699), NASA Goddard Space Flight Center, Greenbelt, MD, USA

[3] Johns Hopkins University Applied Physics Laboratory, Laurel, MD, USA

[4] Department of Biology, Georgetown University, Washington, D.C., USA

[5] Science, Technology, and International Affairs Program, Georgetown University, Washington, D.C., USA

[6] CRESST Center for Research Exploration in Space Science and Technology at the University of Maryland, College Park, MD, USA

[7] Department of Geological Sciences, Arizona State University, Tempe, AZ, USA

[8] Nano-Science Center, Department of Chemistry, University of Copenhagen, Copenhagen, Denmark

[9] SETI Institute, Mountain View, CA, USA

*Corresponding author: 241 Williamson Hall, University of Florida, Gainesville, FL 32611; Email: amywilliams1@ufl.edu

Keywords: Hot springs, Sinter, Fatty acids, TMAH, SAM instrument

Abstract

Hydrothermal spring deposits host unique microbial ecosystems and have the capacity to preserve microbial communities as biosignatures within siliceous sinter layers. This quality makes terrestrial hot springs appealing natural laboratories to study the preservation of both organic and morphologic biosignatures. The discovery of hydrothermal deposits on Mars has called attention to these hot springs as Mars-analog environments, driving forward the study of biosignature preservation in these settings to help prepare future missions targeting the recovery of biosignatures from Martian hot spring deposits. This study quantifies the fatty acid load in three Icelandic hot spring deposits ranging from modern and inactive to relict. Samples were collected from both the surface and 2 to 18 cm in depth to approximate the drilling capabilities of current and upcoming Mars rovers. To determine the preservation potential of organics in siliceous sinter deposits, fatty acid analyses were performed with pyrolysis-GC-MS utilizing thermochemolysis with tetramethylammonium hydroxide (TMAH). This technique is available on both current and upcoming Mars rovers. Results reveal that fatty acids are often degraded in the subsurface relative to surface samples but are preserved and detectable with the TMAH pyrolysis-GC-MS method. Hot spring mid-to-distal aprons are often the only texturally and geomorphically definable feature in older, degraded terrestrial sinter systems and are therefore most readily detectable on Mars from orbital images. These findings have implications for the detection of organics in Martian hydrothermal systems as they suggest that organics might be detectable on Mars in relatively recent hot spring deposits, but preservation likely deteriorates over geologic time scales. Rovers with thermochemolysis pyrolysis-GC-MS instrumentation may be able to detect fatty acids in hot spring deposits if the organics are relatively young; therefore Martian landing site and sample selection are of paramount importance in the search for organics on Mars.

1. Introduction

Siliceous sinter are terrestrial geothermal spring deposits often formed in volcanic settings from silica-supersaturated fluids heated to high temperature by magmatic reservoirs. These fluids rapidly ascend to the surface where the water discharges at geysers and hot spring vents, precipitating silica as the pressure and temperature of the fluids rapidly decrease (Campbell et al., 2015; Renaut and Jones, 2011). The precipitating silica can nucleate and coat all surfaces in the spring discharge flow path, resulting in unique mineralogical textures that are dependent on

Mary Ann Liebert, Inc., 140 Huguenot Street, New Rochelle, NY 10801

temperature and fluid composition when the silica precipitates. Microorganisms that thrive in these extreme temperature, flow rate, and fluid compositions include bacteria, archaea, phages, and eukaryotes (e.g. diatoms) (Breitbart et al., 2004; Leira et al., 2017; Pumas et al., 2018; Saini et al., 2017; Skirnisdottir et al., 2000), and the cells of these organisms can also be entombed by silica precipitation, preserving both the physical structure of the cell as well as cellular organic matter (Cady and Farmer, 1996). These domains of life inhabit specific microenvironments at the hot springs conducive to the organisms' ideal growth conditions. Hyperthermophiles and thermophiles are found near the higher-temperature spring vent, mesophilic organisms such as cyanobacteria inhabit fluids <73 °C between the vent, proximal slope, mid-apron, and distal-apron, and plants and other mesophiles inhabit the lower temperature environments (commonly proximal slope, mid-apron or distal-apron) (Figure 1).

The preservation of organic biosignatures in geothermal spring deposits is of particular interest to the astrobiology community, as several siliceous hot spring deposits have been identified on Mars with both remote sensing and *in situ* exploration. Hydrothermally-driven siliceous sinter deposits have been identified on Mars from orbital observations in Nili Patera (Skok et al., 2010) and Arabia Terra (Allen and Oehler, 2008; Rossi et al., 2008). Hot spring opal-A deposits with nodular and digitate stromatolitic morphologies have been identified in Columbia Hills, Gusev crater, by the *Spirit* rover (Ruff et al., 2011; Squyres et al., 2008), which are strikingly similar to digitate stromatolites with putative biogenic origins found at the El Tatio geothermal field in Chile (Ruff and Farmer, 2016). Although not geothermal in nature, diagenetic silica enrichment is also observed in Marias Pass, Gale crater, by the *Curiosity* rover, which implies groundwater circulation in Gale crater long after lacustrine activity ceased (Frydenvang et al., 2017).

The preservation of physical cells and cellular organic matter in hot springs both constitute biosignatures. Biosignatures are defined as an object, pattern, or substance whose origin specifically requires a biological agent (Hays et al., 2017). Extensive work has been performed that documents the extraordinary preservation of microbial cell structure in sinter deposits by entombment in a very fine matrix of silica particles (Brasier et al., 2011; Cady and Farmer, 1996; Campbell et al., 2015; Guido et al., 2010; Jones et al., 2000; Konhauser et al., 2001; McCollom et al., 2016; Munoz-Saez et al., 2016; Renaut et al., 1998; Tarhan et al., 2016; Walter, 1996; Walter and Des Marais, 1993; Westall et al., 2015; Tobler et al., 2008). Few studies, however, have

Mary Ann Liebert, Inc., 140 Huguenot Street, New Rochelle, NY 10801

focused on the preservation of organic matter in modern and relict (up to 900 year old) siliceous sinter deposits (Chaves Torres et al., 2019; Gibson et al., 2014; Kaur et al., 2015, 2011, 2008; Pancost et al., 2005; Pancost et al., 2006; Teece et al., 2019), and even fewer studies have explored organic preservation potential in Mars-analog hot spring environments (e.g. Williams et al., 2019).

1.1. Martian *In Situ* Organics Detection

The *in situ* search for organic molecules on Mars has been a priority of the scientific community for decades, and several missions have carried payloads with varying organics detection capabilities. The approaches that have been deployed and/or planned to detect organics on Mars missions include Raman spectroscopy (Hays et al., 2017 and references therein), deep UV laser excitation (Hays et al., 2015 and references therein), and gas-chromatography mass-spectrometry (GC-MS). GC-MS has the highest heritage, having flown in modified forms on the Mars Viking landers (Biemann et al., 1977), the Mars Phoenix polar lander (Boynton et al., 2001), and the Sample Analysis at Mars (SAM) instrument on the Mars *Curiosity* rover (Mahaffy et al., 2012). A GC-MS is also included as part of the Mars Organic Molecule Analyzer (MOMA) instrument on the upcoming European Space Agency's *Rosalind Franklin* (ExoMars) rover (Goesmann et al., 2017; Goetz et al., 2016).

The fundamentals of the GC-MS system for all Mars flight instruments are essentially the same: the goal of the approach is to detect and identify various molecular species and classes at low concentrations with high analytic specificity. Volatile compounds thermally evolved from solid samples in an oven may be directly heated (pyrolyzed) or subjected to a derivatization procedure. The evolved species are separated by the GC into a time sequence, then separated by mass and analyzed with the MS. Although pyrolysis GC-MS has the potential to liberate organics bound within mineral matrices, the detection of those organics can be compromised by the presence of perchlorate or other oxidizing salts. Perchlorate is present on the Martian surface and is known to combust organics during pyrolysis due to the evolution of O_2 from the perchlorate, effectively destroying the organic molecule in the process (Guzman et al., 2018). However, certain derivatization or thermochemolysis reactions can liberate and volatilize select organics in the presence of perchlorates without the organics combusting.

A derivatization or thermochemolysis reaction—referred to here, as in the literature, as a "wet chemistry experiment"—is a "one-step" reaction with a reagent that improves organic matter yield

Mary Ann Liebert, Inc., 140 Huguenot Street, New Rochelle, NY 10801

and liberates organics bound within macromolecules. Wet chemistry experiments aim to transform polar organic molecules (e.g. carboxylic acids) into volatile derivatives that are amenable and detectable by GC-MS (del Rio et al., 1996; Metcalffe and Wang, 1981), as well as freeing bound components of larger macromolecules otherwise undetectable with GC-MS (Grasset et al., 2002).

Different wet chemistry reagents can be used based on the chemistry of the targeted labile group and the required yield of the reaction, such as *N,N*-methyltert-butyl-dimethylsilyltrifluoroacetamide (MTBSTFA; (Goesmann et al., 2017; Mahaffy et al., 2012), *N,N*-dimethylformamide dimethyl acetal (DMF-DMA; Goesmann et al., 2017), trimethylsulfonium hydroxide (TMSH; Ishida et al., 1999), and tetramethylammonium hydroxide (TMAH; Grasset et al., 2002; Mahaffy et al., 2012), to name just a few. Thermochemolysis with TMAH in methanol (MeOH, a solvent) allows access to refractory or insoluble organic material, including macromolecular organics such as kerogen-like compounds. Simply pyrolyzing a sample at high temperature (>650°C) results in fragmentation of the parent molecule due to thermal stress, which limits molecule identification. To cleave these refractory molecules at a milder temperature (e.g. ≤600°C), thermochemolysis with TMAH allows the analysis of refractory matter in complex matrices containing low amounts of organic material with minimal destruction of the organic material (Geffroy-Rodier et al., 2009; He et al., 2019; Williams et al., 2019). TMAH thermochemolysis selectively cleaves ester and ether bonds, replacing a labile hydrogen atom with a methyl group (Figure 2), rather than random and uncontrolled thermal decomposition and fragmentation of the organic material (as during pyrolysis). TMAH has been used for several decades in a variety of terrestrial fields of study, including petroleum geochemistry (Larter and Horsfield, 1993), soil science (Chefetz et al., 2000; Deport et al., 2006; Schulten, 1996), and sedimentology (Guignard et al., 2005; Pulchan et al., 1997). TMAH is currently available on the *Curiosity* rover SAM instrument (Mahaffy et al., 2012; Williams et al., 2019) and will also be used on the ExoMars rover MOMA instrument (Goesmann et al., 2017). Fortunately, perchlorate does not substantially affect the recovery of fatty acids liberated with TMAH thermochemolysis (He et al., *submitted*), making TMAH an ideal reagent to use in the search for select organics on Mars. Although the SAM instrument TMAH experiment on the *Curiosity* rover has yet to be performed (as of the time of this writing), several other lines of evidence already indicate that organics are present on the surface and near-surface (<6 cm) of Mars. Chlorinated hydrocarbons such as chlorobenzene and C_2 to C_4 dichloroalkanes were detected in the Sheepbed mudstone in

Mary Ann Liebert, Inc., 140 Huguenot Street, New Rochelle, NY 10801

Yellowknife Bay, Gale crater (Freissinet et al., 2015), and thiophenic, aromatic, and aliphatic organic compounds were found in the 3.5 Gy Murray Formation lacustrine mudstones of Pahrump Hills, Gale crater (Eigenbrode et al., 2018). In more recent SAM experiments, preliminary analyses suggest the presence of select medium-chain alkanes (Freissinet et al., 2019) and medium to high molecular masses, including derivatized molecules (Millan et al., 2019), in samples exposed to SAM's other wet chemistry experiment, derivatization with MTBSTFA (Buch et al., 2006).

These findings represent the first confirmed *in situ* organics detection on Mars, but the source of these organic molecules is uncertain. Abiotic Martian sources (e.g., from atmospheric, hydrothermal, or igneous processes), abiotic exogenous sources such as comets, interplanetary dust particles, or meteorites (Eigenbrode et al., 2018; Freissinet et al., 2015), and life all produce organic molecules. TMAH thermochemolysis, however, provides an unprecedented opportunity to assess the biogenicity of Martian organics, specifically carboxylic and fatty acids. Fatty acids, bound in phospholipids and glycolipids, are abundant and ubiquitous components of eukaryotic and bacterial cellular membranes (Vestal and White, 1989). Carboxylic acids have also been identified in exogenous carbonaceous material, such as in the Murchison meteorite (Cronin et al., 1993). Biotic and abiotic-generated carboxylic acids produce distinctly different profiles in GC-MS analyses. Carboxylic and fatty acids derived from metabolic processes can range from C_2 to $>C_{30}$ in length have an even-over-odd carbon chain length preference due to enzymatically formed acetyl (C_2) units derived from glucose (Volkman, 2006). Abiotic fatty acid patterns will favor shorter carbon chain lengths with no carbon preference (Bray and Evans, 1961; McCollom et al., 1999), although it is important to note that very short chain carboxylic acids can represent metabolic byproducts that were not incorporated into cellular membranes. Therefore, within a certain level of uncertainty, characteristics of a FAME profile could be used to deconvolve the origin of fatty acids detected on Mars (Williams et al., 2019).

The work presented here investigates the preservation and detection of organic molecules, specifically fatty acids, in modern inactive and relict Icelandic hydrothermal spring systems that precipitate siliceous sinter and travertine. Organics preservation in these Mars-analog hot spring environments is compared between mostly inactive and relict spring deposits and include samples from spring vent, mid-apron and distal apron facies, and within a depth range comparable to the sampling depth of the *Curiosity* and future rover drill systems. We present data to assess the limits

Mary Ann Liebert, Inc., 140 Huguenot Street, New Rochelle, NY 10801

of space-flight-like analyses and how returned *in situ* data from extraterrestrial hot springs may be interpreted.

2. Methods

2.1. Sample Locations

Samples were collected at three Icelandic hydrothermal sinter sites, at the surface and subsurface ranging from 2 to 18 cm in depth from spring vent to distal apron, to explore the coupling of system activity with potential preservation of biosignatures. In hydrothermal hot-spring systems there are three main regions: near-vent, the location of higher-temperature fluid discharge from the subsurface; the middle-apron, a moderate temperature region often with pooling water; and the distal-apron, areas of cooler fluid further from the vent (e.g. Figure 1). A currently active region, Hveravellir, sits in the central highlands area of Iceland (Figure 3B) and contains many hot springs and fumaroles. This area is protected as a monument in Iceland, with boardwalks and restricted sites that preserve the formations and minimize human alteration. At Hveravellir, we collected sample 160730.01 (mid-apron) near an active spring vent, but sampling site was only moist and not within the main flow region (Figure 4). We also sampled at a recently inactive vent (160730.09) and the distal-apron (160730.08) of an inactive vent. The pisolith sample (160730.04) had formed in pools at an actively flowing vent. Given the variety of samples from active and recently inactive sites, the Hveravellir system will be referred to as 'inactive' in this work. The geothermally active Hveravellir region has been geochemically characterized, with the spring vents in the area generally emerging at *ca.* 90 °C, with a pH of 8.60 and [SiO_2] of 599 ppm (Camacho, 2017). The actively flowing spring vents proximal to Hveravellir vent sample "160730.09" ranged from 91.0 to 97.1°C, pH 8.15 to 8.65, [SiO_2] of 321 to 641 ppm, and [Cl] of 53.1 to 63.6 ppm. Hveravellir spring waters are considered part of a population of high-temperature geothermal waters, along with Geysir, Hveragerdi, and Reykjadalir, which contain elevated silica concentrations relative to the lower-temperature geothermal regions on the island.

A second site, Gunnuhver, lies on the Reykjanes peninsula in SW Iceland (Figure 3C). The sampling site is recently inactive (no spring activity), but with a large active fumarole ~10 m away and geothermal heat still warming the surface. A downstream (~50 m) channel from the active vent in the Gunnuhver region was 24.1°C with a pH = 7.34. Samples collected at Gunnuhver

Mary Ann Liebert, Inc., 140 Huguenot Street, New Rochelle, NY 10801

included those near-vents, mid- (15 to 23 m) and distal-apron (33 to 49 m) locations from deduced vent locations (Figure 4).

The third site visited was Lýsuhóll, a farmland area with relict sinter deposits and few active vent systems (Figure 3D) with lower temperatures (*ca.* 41°C) and pH = 6.3. Other low temperature (*ca.* 50 °C) thermal springs are present nearby in the Snæfellsnes region (Camacho, 2017). Silica sinter (e.g. Opal-A) deposits constitute the mineralogy of older regions in this deposit, overprinted by younger travertine deposits (Jones and Renaut, 2017, Jones et al., 2005). Vent and near-vent samples were collected at Lýsuhóll. The determination of vent locations was more difficult at this relict site as erosion had disrupted many of the deposits; therefore only three well preserved sites were sampled (Figure 4).

All samples were collected with the appropriate permissions. Hveravellir is a protected natural monument for which we were permitted to sample by the Environment Agency of Iceland. We were permitted to sample the Gunnuhver site by the National Energy Authority. Lýsuhóll is private land for which we had owner permission to sample. Lastly, we also had permission from the Icelandic Institute of Natural History to transport samples out of Iceland.

2.2. Sampling Procedure

To minimize contamination, all sinter samples were collected using solvent-washed and ashed tools, while wearing gloves, facemasks and hairnets. Samples were collected using solvent cleaned (MeOH – MeOH/DCM – DCM) and ashed (at 500°C) chisels, spoons, and tweezers. Rock hammers were covered in a new piece of ashed (at 500°C) foil before use. Samples were placed in solvent washed and ashed (at 500°C) glass jars and stored on ice for transport back to the laboratory. Samples were collected both from the surface (denoted with an 'S') or from several centimeters into the subsurface (denoted with an 'I'). Fresh solvent-washed tools were used for each surface and subsurface sample to limit cross-contamination between sample depths. Samples were transported to the laboratory on ice and stored in a -20 °C freezer upon arrival. Samples for SEM analysis were either collected in the field in sterile whirlpak bags with solvent washed tools, or subsampled in the lab from the solvent washed and ashed glass jars with solvent washed tools.

In the laboratory, sinter from the glass jars was subsampled by breaking off smaller pieces with solvent washed and ashed tweezers. These subsamples were powdered with a solvent washed and

Mary Ann Liebert, Inc., 140 Huguenot Street, New Rochelle, NY 10801

ashed ceramic mortar and pestle and ground for 3 minutes to a homogenous powder. As samples were carefully collected using organically-clean tools and techniques in the field, samples were not treated to remove potential natural external contamination prior to powdering. This follows the approach of Wilhelm et al. (2017).

2.3. Imaging and Mineralogy

The aerial drone maps for Figure 3 was acquired by DJI Mavic Pro with the onboard camera at 12MP resolution. Images were recorded at 2-second intervals to ensure that most surface points would be captured in >5 images. The images were stitched together using the commercially available Pix4D Mapping Software to combine the images into the mosaic. Due to the size of the field sites, map images were acquired at different flight altitudes resulting in the following pixel resolutions: Gunnuhver (5 m, 0.32 cm/pixel), Hveravellir (33 m, 1.41 cm/pixel), and Lýsuhóll (60 m, 2.76 cm /pixel).

Scanning electron microscope (SEM) images of sinter were collected with a Phenom ProX G5 tabletop environmental SEM. Qualitative analyses were conducted using a 3-µm spot size, a beam current of 2.25–2.33 nA, and an accelerating voltage of 15 kV under low vacuum conditions consistent with environment SEM operation.

Mineralogy was determined via X-ray diffraction with either a Bruker D8 Discover X-Ray Diffractometer, (Cu Kα radiation, λ = 1.54059 Å); patterns were acquired from 2-70° 2θ, or an Olympus Terra X-Ray Diffractometer, (Co Kα radiation, λ = 1.78897 Å); patterns were acquired from 5-55° 2θ.

2.4. Pyrolysis GC-MS Conditions for Analog Samples

Aliquots of each powdered sample underwent pyrolysis (with a commercial Frontier pyrolyzer 3030D) GC-MS analysis to measure the distribution and abundance of FAMEs. Ground rock or sediment samples were weighed into non-reactive metal cups (sample mass was ca. 5 to 10 mg, depending on the sample). Just prior to sample analysis, TMAH in the ratio of 1 mg sample to 1 µL TMAH was added to the cup. The *n*-$C_{19:0}$ internal standard was injected into each sample immediately prior to analysis to determine the efficiency of FAME transfer. The sample was then immediately loaded and dropped into the pyrolyzer oven to begin the run. The GC-MS analysis was run on either an Agilent 7890A-5975C inertXL GC-MS or a Thermo Trace 1310 GC-MS equipped with a 30 m Restek capillary column (MXT-5) with a 0.25 mm internal diameter and

0.25 µm thick Crossbond® 5% diphenyl/95% dimethyl polysiloxane stationary phase, and He as the carrier gas at a 3 mL min^{-1} flow rate and 10:1 split. Blank (without TMAH) and "TMAH-blank" (with TMAH) clean up analyses were run between each sample to determine and subtract any background level of residual FAMEs in the column.

Chromatograms and the mass spectra for FAMEs were analyzed with ChemStation software (Agilent Technologies). Identifications were based on comparison to known FAME retention times of a Supelco 37 component FAME mixture that contains saturated FAMEs, monounsaturated fatty acid methyl esters (MUFAMEs), and polyunsaturated fatty acid methyl esters (PUFAMEs) (Sigma-Aldrich). In addition, mass spectra were compared to the National Institute of Standards and Technology (NIST) Spectral Library. Quantifications were based on integration under peaks and scaled to the known amount of the n-$C_{19:0}$ internal standard.

The pyrolyzer and GC programs used are detailed below: For the SAM-like pyrolysis ramp and GC column method, the pyrolyzer program started at 50 °C and was ramped at 35 °C/min to 400 °C with no hold. The inlet program and Tenax ® TA trap started at 15 °C with a 2 minute hold. The inlet was ramped at 68 °C/min to 150 °C and held for 2 minutes, then ramped at 80 °C/min to 305 °C and held for 3 minutes. The GC column program started at 35 °C and was held for 10.9 minutes, then ramped at 15 °C/min to 175 °C with no hold, then ramped at 10 °C/min to 305 °C and held for 1 minute. The auxiliary transfer line was held at 135 °C.

For the 500 °C flash pyrolysis method, the sample was dropped into a 500 °C pyrolyzer oven and held for 1 minute. The inlet program and Tenax ® TA trap started at 15 °C with a 2 minute hold. The inlet was ramped at 900 °C/min to 300 °C and held for 2 minutes. The GC column program started at 35 °C and was held for 2.5 minutes, then ramped at 5 °C/min to 300 °C and held for 5 minutes. The auxiliary transfer line was held at 270 °C.

3. Results

3.1. Mineralogy

The mineralogy of the three sample locations was generally dominated by opal-A, opal-CT, and amorphous silica (Table 1). The modern inactive hot spring vent at Hveravellir was dominantly opal-A with lesser percentages of clinopyroxene, plagioclase, gypsum, and magnesite. Several Hveravellir locations were composed entirely of amorphous silica. The modern inactive hot spring

at Gunnuhver was predominantly opal-CT, with the distal apron being dominantly amorphous silica. This system also contained lesser percentages of halite and quartz. The older relict hot spring at Lýsuhóll is composed almost exclusively of amorphous silica with some minor calcite, and one sample site was composed entirely of calcite.

3.2. FAMEs Detected with 500 °C Instantaneous Flash Pyrolysis

Samples were initially analyzed using a 500 °C flash pyrolysis technique to enable transesterification of fatty acids with TMAH thermochemolysis. Using this technique there was relatively high diversity and abundance of FAMEs in the Hveravellir spring site, a lower diversity and abundance of FAMEs at the inactive Gunnuhver spring site, and diminished diversity and abundance of FAMEs at the Lýsuhóll relict site (Table 2).

At the Hveravellir site, samples were collected from the spring vent, mid-apron, and distal-apron, as well as a pisolith-bearing layer near an active vent. FAMEs detected ranged from *n*-$C_{6:0}$ to *n*-$C_{27:0}$ and included a few monounsaturated fatty acids (MUFAs) and branched *iso*- and *antiso*-$C_{15:0}$ (Figure 5, Table 2). *n*-$C_{16:0}$ and *n*-$C_{18:0}$ were the most abundant FAMEs in all samples, and FAMEs longer than *n*-$C_{18:0}$ were identified at all sites except the vent. In general, the abundance and diversity of FAMEs was increased in the surface samples relative to the subsurface samples, which ranged from 3 to 18 cm in depth. The distal apron sample demonstrated an unexpected general trend of greater FAME concentrations in the interior samples than the surface samples.

At the inactive Gunnuhver site, samples were collected from two spring vents, the mid-apron, and the distal-apron. FAMEs detected ranged from *n*-$C_{4:0}$ to *n*-$C_{276:0}$ and included few MUFAs (Figure 6, Table 2). No methyl-branched fatty acids were detected. Again *n*-$C_{16:0}$ and *n*-$C_{18:0}$ were the most abundant FAMEs in all samples. FAMEs longer than *n*-$C_{18:0}$ were only identified at the mid- and distal-apron sites. In general, the abundance and diversity of FAMEs was increased in the surface samples relative to the subsurface samples, which ranged from 5 to 7 cm in depth.

At the relict Lýsuhóll site, much of the characteristic features of the proximal slope, mid- and distal-aprons were too degraded to assess, so samples were collected from three (near-)vent sites which could be identified in field observations. FAMEs detected ranged from *n*-$C_{6:0}$ to *n*-$C_{27:0}$ and included a few MUFAs and one polyunsaturated fatty acid (PUFA) (Figure 7, Table 2). Methyl-branched *iso*- and *antiso*-$C_{15:0}$ were also detected in the surface and subsurface. Again *n*-$C_{16:0}$ and

n-$C_{18:0}$ were the most abundant FAMEs in most samples, although this is not the case for Vent #1 (160809.03). FAMEs longer than *n*-$C_{18:0}$ were identified at all sites. The abundance and diversity of FAMEs was increased in the surface samples relative to the subsurface samples, which ranged from 2 to 3 cm in depth.

3.3. FAMEs Detected with SAM-Instrument-like Pyrolysis Ramp

Samples were analyzed using a 35°C/min pyrolysis ramp to approximate the pyrolysis ramp used by the SAM instrument on the *Curiosity* rover (Mahaffy et al., 2012; Williams et al., 2019). This technique was utilized to explore how the FAME detection would change if sinter-bearing hot springs were analyzed on Mars with a SAM comparable TMAH experiment. In general, with this technique there was lower diversity and abundance of FAMEs in all three spring systems (Table 3).

At the Hveravellir site, FAMEs detected ranged from *n*-$C_{6:0}$ to *n*-$C_{20:0}$ and included two MUFAs. *n*-$C_{16:0}$ and *n*-$C_{18:0}$ were the most abundant FAMEs in all samples, and only one FAME longer than *n*-$C_{18:0}$ was identified at the surface mid-apron site. In general, the abundance and diversity of FAMEs was equal to or increased in the surface samples relative to the subsurface samples.

At the inactive Gunnuhver site, FAMEs detected ranged from *n*-$C_{4:0}$ to *n*-$C_{2718:0}$ and included several~~one~~ MUFAs and PUFAs. *n*-$C_{16:0}$ and *n*-$C_{18:0}$ were generally the most abundant FAMEs in the mid- and distal-apron samples, and ~~no~~ FAMEs longer than *n*-$C_{18:0}$ were detected in all Gunnuhver samples. ~~No FAMEs larger than *n*-$C_{16:0}$ were detected in the Vent 2 site.~~ The abundance and diversity of FAMEs was ~~uniformly~~ higher in the surface vent samples relative to the subsurface samples, but lower than the subsurface samples from the mid- and distal apron environments~~, with no FAMEs detected in the subsurface Vent 2 sample~~.

At the relict Lýsuhóll site, FAMEs detected ranged from *n*-$C_{4:0}$ to *n*-$C_{18:0}$ and included three MUFAs and one PUFA. *n*-$C_{16:0}$ and *n*-$C_{18:0}$ were the most abundant FAMEs in all samples, and no FAMEs longer than *n*-$C_{18:0}$ were detected. The only site with both a surface and subsurface sample was the 160807.04 Vent #2 location, and the abundance and diversity of FAMEs was higher in the surface sample relative to the subsurface sample.

Mary Ann Liebert, Inc., 140 Huguenot Street, New Rochelle, NY 10801

4. Discussion

The samples studied here comprise silica sinter and calcite hot spring deposits ranging from modern and partially inactive to older, relict spring systems. Thus, they represent a range in geochemistry, mineralogy, age, and diagenetic history, as well as spanning a diversity of subenvironments present in hot spring deposits: vents, mid-aprons, and distal aprons. Despite these differences, several trends in FAME abundance and diversity are shared between the hot spring locations.

A high abundance of n-$C_{16:0}$ and n-$C_{18:0}$ is observed in all of the surface and subsurface samples relative to other FAMEs in all three locations, which is consistent with these two fatty acids being the most common in both bacteria and eukarya (Kaur et al., 2015; Johnson et al., 2019; Wilhelm et al., 2017; Williams et al., 2019). Elevated n-$C_{16:0}$ and n-$C_{18:0}$ FAME abundances relative to other FAMEs are expected in younger sinters versus much older, inactive sinters (Kaur et al., 2011), reflecting more extant diverse microbial communities.

~~Most~~ All samples contain FAMEs longer than *n*-$C_{18:0}$, which most often represent a terrigenous plant or algal origin (Volkman et al., 1989; Kaur et al., 2011; Wilhelm et al., 2017; Johnson et al., 2020), although these fatty acids may be derived from bacterial free, long chain fatty acids (Summons et al., 2013) or intact polar lipids. Based on the abundance of surface vegetation near the spring sites, the FAMEs here are assumed to represent waxy longer chain FAMEs that are often more stable than short chain FAMEs and may be more resistant to diagenetic processes and preserved longer after entombment (Wilhelm et al., 2017). Long chain FAMEs were identified in ~~nearly~~ all surface and subsurface samples. At Hveravellir, they are present in greater abundance at the mid- and distal apron sites than the vent site. At Gunnuhver, long chain FAMEs are ~~also~~ present in the mid- and distal-apron sites, and present at a lower abundance ~~with a noticeable absence~~ in the vent sites. This increase in abundance is consistent with models of lower temperatures (<40°C) downstream from vents, which support plant growth and the potential for their entombment in the sinter (Walter, 1976). At Lýsuhóll these FAMEs are present in the relict vent sites both on the surface and in the subsurface. Much higher concentrations of long chain FAMEs in the surface samples suggest a more modern source. Observation of the long chain FAMEs at depth suggests that plant matter grew and was entrained in the sinter as flow decreased and the spring system cooled and became dormant. The lower concentrations in the subsurface samples indicate some

Mary Ann Liebert, Inc., 140 Huguenot Street, New Rochelle, NY 10801

higher plants were also incorporated into the rock record, with some degradation of the FAMEs due to burial processes.

A strong even-over-odd carbon number preference is consistent with the production of the fatty acids due to enzymatic effects (e.g. the monomer addition of a 2-C sub-unit, (Georgiou and Deamer, 2014; Summons et al., 2008) and of microbial cellular metabolic processes (Elias et al., 1997; Grimalt and Albaiges, 1987; Nishimura and Baker, 1986; Volkman, 2006). All surface and subsurface samples from the Hveravellir site exhibit this trend, as do all surface samples from Gunnuhver.

4.1. Organics Load in the Hveravellir Hot Spring System

The surface FAME load in the Hveravellir spring system varied greatly between the vent, mid-apron, and distal apron facies. The abundance of FAMEs detected with flash pyrolysis at the opal-A vent facies is an order of magnitude (>35000 ng total FAME/ mg TOC) greater than the FAME abundance at the amorphous silica distal apron (ca. 1875 ng total FAME/ mg TOC). The amorphous silica mid-apron FAME abundance was lower still, at ca. 600ng total FAME/ mg TOC. The elevated FAME abundance at the Hveravellir vent sample indicates that the change in water flow and/or temperature at this recently ceased vent has likely led to colonization by bacteria with a lower temperature tolerance. Water flow and temperature are major factors in determining microbial diversity and biofilm texture in hydrothermal systems. When flow shifts, as it has at this vent and outflow system, change to abundance and diversity of the fatty acids should be expected. At the vent, the presence of the C_{20} and C_{22} fatty acids indicate that thermophilic bacterial growth has occurred, however, the relatively high FA abundance, together with an increase in the cyanobacterial $C_{18:\omega9}$ indicates that a reduction in water temperature probably resulted in increased growth of a thermotolerant cyanobacterium such as the high-temperature form of *Mastigocladus* isolated from an Iceland hot spring (Castenholz, 1969) or perhaps diatoms (e.g. Figure 4), or both. This is consistent with the relatively low abundance and lack of $C_{18:\omega9}$ FA in the subsurface sample. As we report on and discuss our results for the sinter samples below it is important to keep in mind that these hydrothermal siliceous springs are dynamic systems suited for the production and preservation of fatty acid, and that under conditions ranging from recent to ancient, fatty acids survive for extended time entombed in siliceous sinter.

Mary Ann Liebert, Inc., 140 Huguenot Street, New Rochelle, NY 10801

~~indicates that lower thermal tolerance bacteria have recolonized this recently ceased vent (i.e. no water flow). The expected trend for an active high-temperature spring system would include a higher fatty acid abundance further from the high temperature vent (Kaur et al., 2011), as a greater diversity of organisms with higher growth rates tend to colonize these regions.~~

The opal-A pisolith layer was collected further away from the other three Hveravellir samples but exhibits a similar trend in even–over-odd carbon number predominance, with *n*-$C_{16:0}$ and *n*-$C_{18:0}$ dominating the FAME profile. Pisoliths are composed of >2 mm diameter spherical concretionary grains called pisolites which are often formed from calcite or amorphous silica. Due to the concretionary nature of the grains, pisolites and related ooids often contain bound organic matter between cortices or submillimeter concretion layers (Davies et al., 1978; Folk and Lynch, 2001; O'Reilly et al., 2017). Therefore, the trends in presence and preservation of FAMEs in the pisolith layer is expected.

The FAME load at Hveravellir changed with depth between the vent, mid-apron, and distal apron facies as well. Most subsurface FAMEs decreased in abundance or were not detected relative to their complementary surface samples (e.g. Figure 8, where the total organic carbon load is generally lower in subsurface samples relative to surface samples). A few exceptions exist in this data set, in particular in the mid-apron sample, in which all of the subsurface FAMEs were elevated in concentration relative to the surface (Figure 5). In the distal-apron samples, several individual subsurface FAMEs were elevated relative to their complementary surface samples. This trend was distinct at the distal apron site, where FAME concentration often increased stepwise from the surface to progressively deeper sampling depths (e.g. Figure 5). We interpret this trend to represent either a temporary increase in organic preservation potential at spring sites that experience lower temperatures and diagenetic alteration, or a modern and robust subsurface microbial community that is generating the elevated FAME abundance. This trend could also be an indication of preservational bias related to differences in mineralization rates, where early mineralization minimizes the degradation of organics and body fossils (Alleon et al., 2016). If a diversion of water flow precipitated a localized temperature shift, the supply of dissolved silica would also decrease leaving the microbial community more vulnerable to biotic and abiotic degradation processes since it was not mineralizing. These observations reinforce the complexity of these spring systems. While general trends can be preserved, changes in the local physical conditions, (like diverted

Mary Ann Liebert, Inc., 140 Huguenot Street, New Rochelle, NY 10801

water flow) can have cascading impacts on the microbial composition and their ecology, that together end up biasing their fossil record.

Although our sampling techniques were optimized to decrease any chance of anthropogenic contamination, we cannot rule out the possibility that some of these samples reflect an anthropogenic influence, as this hot spring is a tourist destination and the mid-apron sample was collected below a visitor boardwalk. Elevated FAMEs from eukaryotic (e.g. human) sources may have been entrained in the sinter. Contamination of this type should yield a much higher FAME concentration, especially in the $C_{16:0}$ and $C_{18:0}$ FAMEs, in the surface relative to the subsurface samples. Surface samples did contain higher concentrations of FAMEs than the subsurface, but $C_{16:0}$ and $C_{18:0}$ FAMEs were not uniformly elevated. Therefore, we interpret the Hveravellir FAME concentration trends as reflecting a diverse and active microbial community.

In general, branched and unsaturated fatty acids were either not detected in subsurface samples or were decreased in abundance relative to the surface samples. This degradation was likely as the unsaturation in the fatty acid is a more reactive location for the molecule to be cleaved by microbial heterotrophy or diagenesis (Killops and Killops, 2005; Sun et al., 1997). A decrease in unsaturated fatty acids and branching is documented in older sinter samples (Kaur et al., 2011) and is consistent with the expectation for preferential degradation of unsaturated fatty acids. However, this trend was reverse in the mid-apron sample, in which all of the subsurface FAMEs, including branched and MUFAs were elevated in concentration relative to the surface.

4.2. Organics Load in the Gunnuhver Hot Spring System

The surface FAME load in the inactive Gunnuhver spring system also varied between the vent, mid-apron, and distal apron facies, although to a lesser degree than in the Hveravellir spring system. The abundance of FAMEs detected with flash pyrolysis is comparable between the opal-CT vent and opal-CT mid-apron facies (ca. 18,000 to 20,000 ng total FAME/ mg TOC) and is elevated in the amorphous silica distal apron facies (ca. 37000 ng total FAME/ mg TOC). This trend in abundance is expected, as a greater diversity of organisms with higher growth rates tend to colonize lower temperature geothermal regions such as the distal apron.

The abundance and diversity of lower molecular weight FAMEs increases to the mid-apron and distal apron facies relative to the vent facies, suggesting that higher molecular weight (longer)

Mary Ann Liebert, Inc., 140 Huguenot Street, New Rochelle, NY 10801

FAMEs are not less well preserved further from the vent and are likely degraded to shorter chains, potentially due to microbial heterotrophy.

The FAME load in this system changed with depth more dramatically than in the Hveravellir system. Subsurface FAME abundance decreases substantially or to no detection relative to their complementary surface samples, indicating continued degradation of the FAMEs in the subsurface due to diagenesis and microbial recycling. Only four FAMEs (n-$C_{8:0}$, n-$C_{10:0}$, n-$C_{15:0}$ and *trans*-$C_{18:1}$) are detected in the subsurface distal apron site with flash pyrolysis(~~n-$C_{8:0}$, n-$C_{10:0}$, n-$C_{15:0}$ and *trans*-$C_{18:1}$~~). The subsurface FAME profiles exhibit strong to weak even-over-odd trends in carbon number. The subsurface distal apron sample does not exhibit any trends in carbon number or molecular weight, which likely reflect whole-scale degradation of all FAMEs in the subsurface. Mono- and polyunsaturated fatty acids are already limited in detection at the surface, a dearth that continues into the subsurface and indicates preferential degradation of the unsaturated FAMEs. Branched fatty acids are not detected in ~~n~~either the surface ~~n~~or subsurface samples with flash pyrolysis.

4.3. Organics Load in the Lýsuhóll Hot Spring System

In contrast with the opal and amorphous silica-dominated Hveravellir and Gunnuhver sites, the Lýsuhóll relict spring system is composed of both amorphous silica and calcite, with Vent #3 composed entirely of calcite. The spring waters that precipitate these deposits, and the subsequent microbial communities that colonize the springs, may be different from those present in the siliceous sinter deposits (Zhang et al., 2004). Additionally, several samples from the relict Lýsuhóll system were destroyed and/or contaminated during transport back to the United States, reducing the completeness of the surface versus subsurface samples originally collected at these sites. Regardless, several conclusions can be drawn from the remaining samples about the organics load in this relict system. All sample sites at Lýsuhóll represented near-vent environments as these were the most readily identified in older, degraded hot spring deposits. The surface FAME load in the relict Lýsuhóll system also varied between the vent facies, ranging from *ca.* 3,700 ng total FAME/ mg TOC in the amorphous silica and calcite dominated Vent #2, to *ca.* 350 ng total FAME/ mg TOC in the amorphous silica Vent #1, to *ca.* 83 ng total FAME/ mg TOC in the calcite Vent #3 (Table 2). As in the other spring systems, the surface FAME concentrations are higher than in subsurface samples. The total FAME abundance ranges from ca. 3700 ng total FAME/ mg TOC

in the Vent 160807.04 (Vent #2) surface sample to ca. 1500 ng total FAME / mg TOC in the complementary subsurface sample. This indicates continued degradation of the FAMEs in the subsurface due to diagenesis and microbial recycling. The Lýsuhóll samples exhibit a moderate to weak even-over-odd preference, which may indicate degradation of fatty acids from the original microbial community, and limited input of organics from a modern community. The relict Lýsuhóll system is the only site where the PUFA *trans*-$C_{18:2}$ algal biomarker is detected (Campbell et al., 2015), and then only in two subsurface samples. Branched and unsaturated fatty acids are already limited in detection at the surface, a dearth that continues into the subsurface and indicates preferential degradation of these fatty acids.

4.4. Comparison between Flash Pyrolysis and Flight-like Ramp Pyrolysis

The 500 °C flash pyrolysis method, combined with TMAH thermochemolysis, represents a laboratory-optimum method to release organics bound within macromolecules and sorbed to minerals. The SAM instrument on the *Curiosity* rover, while able to perform similar experiments, is limited to a 35°C/ min pyrolysis ramp. To assess how this method variation might affect the detection of FAMEs in these Mars-analog siliceous sinters, samples were analyzed with the SAM-like 35°C/ min pyrolysis ramp.

The flash pyrolysis method improved FAME detection uniformly across the sample suite (Figure 8), and with few ~~one~~ exceptions, FAMEs >*n*-$C_{18:0}$ were only detected with the flash method. The ramp method released between 30 and 86% of the FAMEs detected in the flash method. ~~Two outliers to this data set include sample 160727.03.I (200% improvement in the ramp versus flash method) and 160727.02.I (no fatty acids liberated using the ramp method).~~ Although the flash method is more efficient at FAME release, it is promising for the search for organics on Mars that FAMEs are also detectable with the SAM instrument pyrolysis ramp rate.

Correlations vary between the number of FAMEs detected, the concentration of FAMEs in the sample suite. In the Hveravellir system, the greatest diversity of FAMEs detected was generally correlated with low % TOC. This diversity is invaluable in assessing microbial community composition, even at low concentrations. In the inactive spring system, the greatest diversity of FAMEs correlates with higher % TOC, which represents an anticipated trend with regards to FAME preservation (and degradation), FAME diversity and concentration, and the total organic carbon load in the sample (Table 1). The greatest diversity of FAMES was detected in the relict

Mary Ann Liebert, Inc., 140 Huguenot Street, New Rochelle, NY 10801

spring system, as were some of the highest % TOC values. In particular, *n*-$C_{16:0}$ concentrations were predictably low in the subsurface samples and high in the surface samples. These lines of evidence indicate the relict system is experiencing higher delivery of organic load now than it perhaps did in the past. The organics that constitute these higher % TOC values may represent a far greater diversity of organic molecules than just fatty acids, which are preserved but in low concentrations in the relict system.

4.5. Mineralogic Evolution and the Preservation of Organic Matter

It is important to note that the primary controls on lipid preservation in siliceous sinter deposits are thermal alteration, high temperatures, and the pH of each spring (Kaur et al., 2015; Pancost et al., 2006), which can vary greatly between spring systems. A great variety of lipid biomarkers have been identified in modern to *ca*. 900 year old geothermal environments (Jahnke et al., 2001; Shiea et al., 1991; Pancost et al., 2005, 2006; Zhang et al., 2007, Kaur et al., 2011). Often branched or unsaturated fatty acids are prevalent in younger deposits (Kaur et al., 2011), as was also demonstrated in the work presented here. In an actively flowing spring system, temperature in particular tends to ~~drive~~ strongly influence the length and therefore abundance of ~~fatty acids~~hydrocarbons, such as bacterial diethers in active geothermal systems (Kaur et al., 2015). Thermophilic organisms tend to have ~~longer~~ higher molecular weight diethers with higher thermostabilities, longer fatty acid chains (Oshima and Miyagawa, 1974; Russell, 1984; Weerkamp and Heinen, 1972), increased ~~the~~ ratios of *iso*- to *anteiso*-branched fatty acids (Oshima and Miyagawa, 1974; Shen et al., 1970), and fewer unsaturations and branches (Daron, 1970; Ray et al., 1971). All of these adaptations serve to maintain optimal membrane fluidity at higher temperatures.

Although the Hveravellir vent sampled here was no longer actively flowing, several of these trends were observed (Figure 9), consistent with the recent cessation of flowing spring water. The average chain length ranges from 15.1 to 16.4 for all surface and subsurface Hveravellir samples, with the exception of the surface vent sample with an ACL of 13.6. These values suggest that the surface vent microbial community and/or FAME preservation is different from the other surface and subsurface samples at Hveravellir. The low ACL value of the surface vent suggests that this spring vent never experienced very high fluid temperatures and even if thermophilic organisms were present, their organic biosignatures are not well preserved. An increase in heterotrophy may have

Mary Ann Liebert, Inc., 140 Huguenot Street, New Rochelle, NY 10801

occurred concurrent with the cessation of water activity that hosted the thermophiles. The ratio of *i*- to *a*-C_{15} is elevated near the vent where elevated temperatures affect community composition and the *iso* to *anteiso* ratio trend was consistent at this site between the surface and subsurface samples. Additionally, the ratio of branched to total fatty acids increases with distance from the higher temperature vent, consistent with a decrease in the dominance of any thermophilic organisms.

In contrast, the inactive Gunnuhver site had a relatively consistent, elevated total FAME concentration at the vent and mid-apron facies, and a much higher FAME concentration at the distal apron facies, consistent with secondary recolonization of the sinter by more diverse, lower temperature mesophiles after spring flow ceased. Average chain length also decreases from the vent facies (ACL = 10.7 to 13.4 at vents) to the distal apron facies (ACL = 0 to 8.9), suggesting the degradation of fatty acids to shorter chains due to heterotrophy or diagenesis.

Only relict inactive vents were sampled at the Lýsuhóll spring site, which allows a comparison with the modern inactive vent systems. The total FAME concentrations at the relict site was within the range of the inactive spring sites, with higher abundances in the surface samples and lower abundances in the subsurface samples. Average chain length at the relict site (ACL = 14.9 to 17.4) is within the range of the Hveravellir spring site, suggesting that these Lýsuhóll vents were higher temperature when flowing and the thermophile FAMEs are well preserved. The *iso* to *anteiso* ratio was lower than at the modern inactive spring sites, suggesting degradation of the branched fatty acids from an original, higher temperature population. The ratio of branched to total fatty acids, however, was comparable to or higher than the Hveravellir vent site, indicating that more branched fatty acids relative to the total fatty acid load are preserved. This trend may be due to a greater initial branched fatty acid load that, along with the total fatty acids, has experienced degradation. The branched to total fatty acid ratio at Vent #3 (160807.12) is higher than all other samples and contains the longest ACL of all samples from this study. This vent is composed solely of travertine, which may introduce a preservation bias between this younger calcite deposit and the other vents that are older and silica-dominated. The high branched to total fatty acid ratio and ACL value of Vent #3 may also correspond to an active mesophilic microbial community at this site.

Low temperature degradative processes such as heterotrophy and diagenesis control the fatty acid distribution observed in this study. The primary fatty acid distribution from thermophilic versus mesophilic communities is discernable in some environments (e.g. Hveravellir vent) but not

Mary Ann Liebert, Inc., 140 Huguenot Street, New Rochelle, NY 10801

diagnostic of more specific temperature and pH conditions of each subenvironment at each spring system. The vents from the three systems studied here are compared to assess the preservation of organics as a concentration of FAMEs in the surface and subsurface (Figure 10). Additional work can be completed to assess the preserved lipids separate from modern lipids in all three systems, including solvent washing sinter samples to remove surface lipids prior to analysis. At the recently inactive Hveravellir vent (sample 09), the C_{16} and C_{18} FAMEs are likely elevated due to these being the dominant FAMEs in both bacteria and eukarya, although anthropogenic influences, especially in the surface sample, cannot be completely dismissed. The lower concentrations of the other FAMEs in the surface and subsurface reflect a nominal FAME profile from an active microbial community, with the expected even-over-odd carbon number preference. The inactive Gunnuhver vent generally had the lowest FAME concentrations relative to the Hveravellir and Lýsuhóll systems, but still exhibited the even-over-odd carbon number preference characteristic of an active microbial community. The low FAME concentrations reflects FAME degradation leading to low preservation potential, and a lack of extensive recolonization of the sinter by secondary microbial communities. The higher FAME concentrations at the relict Lýsuhóll Vent #2 (especially relative to the inactive Gunnuhver site) likely reflect microbial (re)colonization by a community distinct from that found in active/recent silica-precipitating hot springs. The mixed amorphous silica and calcite mineralogy of this vent likely also contributes to this marked difference in FAME abundance.

The mineralogic evolution and diagenesis of siliceous hot spring sinters is well studied (Herdianita et al., 2000). Initial silica precipitates are composed of amorphous silica or opal-A (Tobler et al., 2017), and the very fine size of these precipitates are documented to preserve microbial cells in extraordinary physical detail (Cady and Farmer, 1996; Jones et al., 2000; Renaut et al., 1998), although progressive silicification and preservation biases over long time scales can also destroy these physical biosignatures (Jones et al., 1997; Jones and Renaut, 1996). As siliceous sinter deposits experience diagenesis, opal-A incrementally recrystallizes to Opal-C (containing disordered α-cristobalite) or opal-CT (containing cristobalite and tridymite). This transition may occur on the order of *ca.* 50 years up to tens of thousands of years. Over longer time scales (*ca.* 10,000 to 50,000 years), opal-C/ -CT will reorder to microcrystalline quartz. Although sinter age can sometimes be used as an estimate for crystallinity, variables such as fluid mobilization and composition can also greatly affect crystallinity (Herdianita et al., 2000). This recrystallization

process, and specifically the transition to microquartz, reduces porosity and decreases the preservation of organic matter in siliceous sinter (Teece et al., 2020).

These trends in mineralogy and organics preservation were upheld in the current study. In the Hveravellir system, which is composed of amorphous silica and opal-A, the diversity and abundance of FAMEs was elevated in both the surface and subsurface. In contrast, the inactive Gunnuhver system, which is composed primarily of opal-CT, had a much lower diversity and abundance of preserved FAMEs. Lynne et al. (2006) suggest that silica diagenesis is accelerated in hot spring systems that have transformed from flowing water to steam dominated. The transformation to opal-CT in this relatively young system was likely controlled by fluid composition and fluid or steam mobilization. This mobilization led to accelerated diagenesis and fumarolic degradation of organics in the Gunnuhver system. The surprisingly elevated diversity and abundance of FAMEs in the relict Lýsuhóll system was controlled in part by the mineralogy, which is dominated by calcite and amorphous silica, as well as a modern microbial community that had colonized the surface of this deposit. These results further reinforce the importance of ascertaining sample mineralogy prior to sampling for organics in hydrothermal systems, especially on life detection missions beyond Earth.

4.6. Biomarker Preservation and Implications for Organics Detection on Mars

The size and distribution of hot spring facies varies across systems, yet trends in preservation styles, from the outcrop- to the submicrometer scale, are present and can be used to provide depositional context as we continue to explore life in other planets. On Earth, preservation at the vent is often less favorable with microfossils usually in the form of smaller diameter molds that can be readily infilled and obscured (Cady and Farmer, 1996). Vents may be identified by finely laminated deposits in a circular form that are often associated with geyserite. The directed water flow in channel facies produces bacterial streamer fabrics, long filaments parallel to water direction, sometimes composed of cyanobacterial filaments (Parenteau et al., 2014). This streamer morphology is readily identified in outcrop (e.g., Parenteau et al, 2014, Walter et al., 1998). The lower temperatures of the distal apron are usually accompanied by thick microbial mats creating palisade fabrics with abundant microfossils and organics that can be preserved (Cady and Farmer, 1996; Campbell et al., 2015). Apron facies are one of the better-preserved lithofacies in degraded spring systems, with the mid-to-distal apron composing the largest aerial extent, followed by the

Mary Ann Liebert, Inc., 140 Huguenot Street, New Rochelle, NY 10801

channel facies and then vent facies. Based solely on aerial extent, Martian hot spring apron facies may be most easily detected from orbital imaging and targeted for *in situ* exploration.

Biosignature preservation within all facies is complicated by preservation bias and diagenesis over geologic time scales. Even the proximal slopes and aerially extensive mid- and distal-aprons may become challenging to identify as the fine scale micro-textures that define these spring sub-environments can be lost to diagenesis and preservation biases (Cady and Farmer, 1996). Although diagenesis can and does obscure some features, the apron facies contain structures such as pools and terracettes that are identifiable in surface deposits and layered deposits with palisade fabric identifiable in outcrop cross-section. Vents are just as prone to erosion and infilling (this was observed at Lýsuhóll and Gunnuhver), and with a much smaller footprint, can be challenging to identify from orbital images. However, the primary macro-scale textural characteristics of spring vents can enable their identification after some geologic reworking (Cady and Farmer, 1996, and references therein).

Given these complexities, it is therefore important to develop a facies-oriented understanding of biosignature preservation potential in terrestrial hot springs to better predict the ideal locations to search for organics in Martian relict hydrothermal spring systems. The temperature of fluids at subaerial hydrothermal vent systems can vary greatly, up to or above surface boiling temperatures. Non-photosynthetic microbes can live in these temperatures, with hyperthermophiles preferring >80 °C up to a maximum of 110 °C where elevated hydrostatic pressure allows waters to reach higher temperature without boiling (Segerer et al., 1993). For reference, the upper temperature limit for archaeal life is 121 °C in submarine black smoker environments (Kashefi and Lovley, 2003); in contrast, photosynthetic microbes are present in waters below 73 °C (Ward et al., 2012). Although these organisms do not directly contribute to silica precipitation in these spring systems, they can be entombed and preserved in the rapidly precipitating silica, contributing to the organic load and microstructures found in near-vent environments (Cady and Farmer, 1996). In our study, silicified traces of microorganisms are readily identified in SEM images from the Hveravellir and Lýsuhóll sample sites, but no distinct biogenic features were identified from the Gunnuhver sinter samples (Figure 4). These observations appear to correlate with the relative abundances of organics detected at these three locations.

The search for (biogenic) organic molecules on Mars' near-surface requires new and novel techniques to detect these molecules with miniaturized space-flight payloads. In the terrestrial realm, many biomarkers are preserved and detectable in siliceous sinter environments with laboratory instrumentation such as off-line lipid fraction extraction, derivatization and/or saponification, followed by multiple GC-MS and/or liquid chromatography-mass spectrometry (LC-MS) analyses. However, suites of these laboratory techniques are often too complex to be successfully miniaturized for space-flight and remote operation. Therefore, "one-step" thermochemolysis or derivatization pyrolysis GC-MS is an optimized technique that is miniaturized to work on space-flight missions such as with the SAM and MOMA instruments. To be more "SAM-like" in this study, samples that may contain low-temperature surface biofilms were collected and ground as whole rock samples in a manner similar to *Curiosity's* sample acquisition system. Therefore, the results from this study likely reflect a greater abundance of organics than may be expected to be preserved in a Martian hot spring deposit with a hypothetical microbial community. Although more diagnostic biomolecules are present in Mars-analog hydrothermal spring environments, this work demonstrates that FAMEs are preserved and detectable with space-flight-like GC-MS techniques in modern inactive and relict siliceous sinter and calcite deposits from Iceland. The MOMA instrument on the *Rosalind Franklin* rover will be able to ramp the pyrolysis oven at >200 °C/min (from thermal vacuum), achieving a much faster ramp than the SAM instrument and perhaps increasing the likelihood of detecting Martian FAMEs, if present.

The rate of siliceous sinter formation, hydrothermal conditions, and those effects on biomass growth and potential for silicification in each individual Icelandic sinter deposit reflect differences in the diversity and abundance of biomolecules detected in this work. The geologic process of a hot spring becoming quiescent should be similar on Earth and Mars. The evolution of a putative microbial community within that hot spring can be approximated in specific ways by assessing microbial community evolution in hot springs on Earth. The approximations ~~by definition require~~require assumptions that do not account for Mars-specific conditions such as atmospheric composition, radiation flux, energy sources, etc. By assessing the microbial communities and preserved organics from lower temperature inactive and relict spring systems, this work approximates the organics load in Martian hot springs with a hypothetical microbial community that would have evolved as the spring system cooled to dormancy. Understanding the distribution

Mary Ann Liebert, Inc., 140 Huguenot Street, New Rochelle, NY 10801

of organics in terrestrial systems is vital for choosing an ideal Martian hydrothermal target for organic biosignature exploration.

A final consideration in the search for organics on Mars is the deleterious effects of oxidants and radiation on organics. Although organic matter has been identified in Mars near-surface substrates with the SAM instrument (Eigenbrode et al., 2018; Freissinet et al., 2015), fewer molecules detected by SAM represent reduced carbon, with many of these organics being oxidized. For example, polycyclic aromatic hydrocarbons (PAHs) and kerogen from exogenous delivery via meteoritic infall may undergo several oxidation reactions to form stable simple organics such as phthalic, mellitic, or oxalic acids (Benner et al., 2000; Freissinet et al., 2015) on the Martian surface, which are then detectable by the SAM instrument (e.g. possible source organics for benzene in the Sheepbed mudstone, Freissinet et al. (2015)). These oxidation processes are expected to occur both on the surface and in the subsurface of Mars.

Ionizing radiation is another serious concern for the long-term preservation of Martian organics. The ionizing radiation dose on the surface of Mars is estimated at 0.54–0.85 Gray/year (Dartnell et al., 2007). Ionizing radiation destroys biomolecules (e.g. proteins or DNA), and most bacteria cannot survive doses greater than 200 Gray (Daly, 2009). Recent studies indicate that within 300 million years, preservation of functionalized organic molecules greater than 500 amu in the top ~5 cm of rock drops 1000x due to ionizing radiation (Pavlov et al., 2012). There is some indication that rapid burial of organics, short exposure ages due to relatively slow Martian weathering rates, and the characteristics of some entombing mineralogies may assist in organics preservation in the Martian near-surface (Hays et al., 2017 and references therein), but the need remains to sample the Martian subsurface to reduce the impact of degradation via radiation effects.

The *Curiosity* rover can drill to a maximum of six centimeters and the *Rosalind Franklin* rover will be able to drill to two meters depth. The work presented here indicates that even with diagenetic effects and heterotrophic cycling of organics, organic molecules are preserved and detectable over short timescales in the near-subsurface (2 to 18 cm in depth) of modern and relict terrestrial hot springs. Organics therefore may be detectable on Mars in relatively recent hot spring deposits, but preservation likely deteriorates over geologic time scales. These depths are within the drill sampling range of the *Curiosity* and *Rosalind Franklin* rovers (partial to complete depths,

Mary Ann Liebert, Inc., 140 Huguenot Street, New Rochelle, NY 10801

respectively), and support the search for near-surface organics preserved in Martian hydrothermal systems.

5. Conclusions

Hydrothermal spring deposits host unique microbial ecosystems and have the capacity to physically preserve both microbial communities and their associated organic matter as biosignatures within siliceous sinter. These terrestrial geothermal springs serve as Mars analog environments to prepare future Mars missions to target their search for biosignatures in Martian hot spring deposits. This study quantified the preservation and detectability of fatty acids in three Icelandic hot spring deposits ranging from modern and inactive to relict, and samples were collected both at the surface and at depth (ranging from 2 to 18 cm in depth). Analyses performed with TMAH thermochemolysis pyrolysis-GC-MS indicate that fatty acids were preserved and detectable in all three spring deposits, with the subsurface samples degraded relative to the surface samples. TMAH thermochemolysis pyrolysis-GC-MS analyses using a SAM-instrument-like procedure were also successful in liberating preserved fatty acids from these sinter samples, albeit generally in lower abundances and with less diversity. These results build confidence in our ability to detect fatty acids and distinguish biogenicity using the GC-MS instrumentation available on current and future Mars missions.

6. Acknowledgements

Financial support for sample collection was provided by the NASA Planetary Science and Technology through Analog Research (PSTAR) program grant #NNX15AJ38G to J.R. Skok and the American Philosophical Society's Lewis and Clark Fund for Exploration and Field Research in Astrobiology to K. Craft. S.S. Johnson would like to acknowledge support from NASA grant #NNX17AJ68G ("Using Organic Molecule Detections in Mars Analog Environments to Interpret the Results of the SAM Investigation on the Mars Science Laboratory Mission") as well as a Georgetown University Pilot Research Grant.

7. Author Disclosure Statement

No competing financial interests exist.

Mary Ann Liebert, Inc., 140 Huguenot Street, New Rochelle, NY 10801

8. References

Allen, C.C., Oehler, D.Z., 2008. A Case for Ancient Springs in Arabia Terra, Mars. Astrobiology 8, 1093–1112. https://doi.org/10.1089/ast.2008.0239

Benner, S.A., Devine, K.G., Matveeva, L.N., Powell, D.H., 2000. The missing organic molecules on Mars. Proc. Natl. Acad. Sci. 97, 2425 LP – 2430. https://doi.org/10.1073/pnas.040539497

Biemann, K., Oro, J., Toulmin, P., Orgel, L.E., Nier, A.O., Anderson, D.M., Simmonds, P.G., Flory, D., Diaz, A. V., Rushneck, D.R., Biller, J.E., Lafleur, A.L., 1977. The search for organic substances and inorganic volatile compounds in the surface of Mars. J. Geophys. Res. 82, 4641–4658. https://doi.org/10.1029/JS082i028p04641

Boynton, W. V., Bailey, S.H., Hamara, D.K., Williams, M.S., Bode, R.C., Fitzgibbon, M.R., Ko, W., Ward, M.G., Sridhar, K.R., Blanchard, J.A., Lorenz, R.D., May, R.D., Paige, D.A., Pathare, A. V., Kring, D.A., Leshin, L.A., Ming, D.W., Zent, A.P., Golden, D.C., Kerry, K.E., Lauer, H.V., Quinn, R.C., 2001. Thermal and Evolved Gas Analyzer: Part of the Mars Volatile and Climate Surveyor integrated payload. J. Geophys. Res. Planets 106, 17683–17698. https://doi.org/10.1029/1999JE001153

Brasier, M.D., Antcliffe, J.B., Callow, R.H., 2011. Evolutionary trends in remarkable fossil preservation across the Ediacaran–Cambrian transition and the impact of metazoan mixing, in: Taphonomy. Springer, Dordrecht, pp. 519–567.

Bray, E., Evans, E., 1961. Distribution of n-paraffins as a clue to recognition of source beds. Geochim. Cosmochim. Acta 22, 2–15.

Breitbart, M., Wegley, L., Leeds, S., Schoenfeld, T., Rohwer, F., 2004. Phage Community Dynamics in Hot Springs. Appl. Environ. Microbiol. 70, 1633 LP – 1640. https://doi.org/10.1128/AEM.70.3.1633-1640.2004

Buch, A., Glavin, D.P., Sternberg, R., Szopa, C., Rodier, C., Navarro-González, R., Raulin, F., Cabane, M., Mahaffy, P.R., 2006. A new extraction technique for in situ analyses of amino and carboxylic acids on Mars by gas chromatography mass spectrometry. Planet. Space Sci. 54, 1592–1599. https://doi.org/https://doi.org/10.1016/j.pss.2006.05.041

Cady, S.L., Farmer, J.D., 1996. Fossilization processes in siliceous thermal springs: trends in preservation along thermal gradients. Evol. hydrothermal Ecosyst. Earth (and Mars?) 150–173. https://doi.org/10.1002/9780470514986.ch9

Campbell, K.A., Lynne, B.Y., Handley, K.M., Jordan, S., Farmer, J.D., Guido, D.M., 2015. Tracing Biosignature Preservation of Geothermally Silicified Microbial Textures into the Geological Record. Astrobiology 15, 858–882. https://doi.org/10.1089/ast.2015.1307

Castenholz, R.W., 1969. THE THERMOPHILIC CYANOPHYTES OF ICELAND AND THE UPPER TEMPERATURE LIMIT. J. Phycol. 5, 360–368. https://doi.org/10.1111/j.1529-8817.1969.tb02626.x

Chaves Torres, L., Kaur, G., Melbourne, L.A., Pancost, R.D., 2019. Selective chemical degradation of silica sinters of the Taupo Volcanic Zone (New Zealand). Implications for early Earth and Astrobiology. Geobiology 0, 1–16. https://doi.org/10.1111/gbi.12340

Chefetz, B., Chen, Y., Clapp, C.E., Hatcher, P.G., 2000. Characterization of organic matter in soils by thermochemolysis using tetramethylammonium hydroxide (TMAH). Soil Sci. Soc. Am. J. 64, 583–589.

Cronin, J.., Pizzarello, S., Epstein, S., Krishnamurthy, R.., 1993. Molecular and isotopic analyses of the hydroxy acids, dicarboxylic acids, and hydroxydicarboxylic acids of the Murchison meteorite. Geochim. Cosmochim. Acta 57, 4745–4752. https://doi.org/10.1016/0016-7037(93)90197-5

Daly, M.J., 2009. A new perspective on radiation resistance based on Deinococcus radiodurans. Nat. Rev. Microbiol. 7, 237–245. https://doi.org/10.1038/nrmicro2073

Daron, H.H., 1970. Fatty acid composition of lipid extracts of a thermophilic Bacillus species. J. Bacteriol. 101, 145–151.

Dartnell, L.R., Desorgher, L., Ward, J.M., Coates, A.J., 2007. Modelling the surface and subsurface Martian radiation environment: Implications for astrobiology. Geophys. Res. Lett. 34, 1–6. https://doi.org/10.1029/2006GL027494

Davies, P.J., Bubela, B., Ferguson, J., 1978. The formation of ooids. Sedimentology 25, 703–730.

del Rio, J.C., Martin, F., Gonzalez-Vila, F.J., 1996. Thermally assisted hydrolysis and alkylation as a novel pyrolytic approach for the structural characterization of natural biopolymers and geomacromolecules. Trends Anal. Chem. 15, 70–79.

Deport, C., Lemee, L., Ambles, A., 2006. Comparison between humic substances from soil and peats using TMAH and TEAAc thermochemolysis. Org. Geochem. 37, 649–664.

Eigenbrode, J.L., Summons, R.E., Steele, A., Freissinet, C., Millan, M., Navarro-González, R., Sutter, B., McAdam, A.C., Franz, H.B., Glavin, D.P., Archer, P.D., Mahaffy, P.R., Conrad, P.G., Hurowitz, J.A., Grotzinger, J.P., Gupta, S., Ming, D.W., Sumner, D.Y., Szopa, C., Malespin, C., Buch, A., Coll, P., 2018. Organic matter preserved in 3-billion-year-old mudstones at Gale crater, Mars. Science (80-.). 360, 1096–1101. https://doi.org/10.1126/science.aas9185

Elias, V., Simoneit, B., Cardoso, J., 1997. Even N-Alkane Predominances on the Amazon Shelf and A Northeast Pacific Hydrothermal System. Naturwissenschaften 84, 415–420.

Folk, R.L., Lynch, F., 2001. Organic matter, putative nannobacteria and the formation of ooids and hardgrounds. Sedimentology 48, 215–229.

Freissinet, C., Glavin, D.P., Buch, A., Szopa, C., Teinturier, S., Archer, P.D., Williams, R., Millan, M., Williams, A.J., Malespin, C., Mahaffy, P., 2019. Detection of long-chain hydrocarbons on mars with the Sample Analysis at Mars (SAM) instrument, in: Mars 9 Conference. p. 6123.

Freissinet, C., Glavin, D.P., Mahaffy, P.R., Miller, K.E., Eigenbrode, J.L., Summons, R.E., Brunner, A.E., Buch, A., Szopa, C., Archer, P.D., Franz, H.B., Atreya, S.K., Brinckerhoff, W.B., Cabane, M., Coll, P., Conrad, P.G., Marais, D.J. Des, Dworkin, J.P., Fairén, A.G., François, P., Grotzinger, J.P., Kashyap, S., Kate, I.L., Leshin, L.A., Malespin, C.A., Martin, M.G., Mcadam, A.C., Ming, D.W., Pavlov, A.A., Prats, B.D., Squyres, S.W., Steele, A., Stern, J.C., Sumner, D.Y., Sutter, B., Zorzano, M., 2015. Organic molecules in the Sheepbed Mudstone, Gale Crater, Mars. J. Geophys. Res. 120, 495–514. https://doi.org/10.1002/2014JE004737.Received

Frydenvang, J., Gasda, P.J., Hurowitz, J.A., Grotzinger, J.P., Wiens, R.C., Newsom, H.E.,

Edgett, K.S., Watkins, J., Bridges, J.C., Maurice, S., Fisk, M.R., Johnson, J.R., Rapin, W., Stein, N.T., Clegg, S.M., Schwenzer, S.P., Bedford, C.C., Edwards, P., Mangold, N., Cousin, A., Anderson, R.B., Payré, V., Vaniman, D., Blake, D.F., Lanza, N.L., Gupta, S., Van Beek, J., Sautter, V., Meslin, P.-Y., Rice, M., Milliken, R., Gellert, R., Thompson, L., Clark, B.C., Sumner, D.Y., Fraeman, A.A., Kinch, K.M., Madsen, M.B., Mitrofanov, I.G., Jun, I., Calef, F., Vasavada, A.R., 2017. Diagenetic silica enrichment and late-stage groundwater activity in Gale crater, Mars. Geophys. Res. Lett. 44, 4716–4724. https://doi.org/10.1002/2017GL073323

Geffroy-Rodier, C., Grasset, L., Sternberg, R., Buch, A., Amblès, A., 2009. Thermochemolysis in search for organics in extraterrestrial environments. J. Anal. Appl. Pyrolysis 85, 454–459. https://doi.org/https://doi.org/10.1016/j.jaap.2008.10.005

Georgiou, C.D., Deamer, D.W., 2014. Lipids as Universal Biomarkers of Extraterrestrial Life. Astrobiology 14, 541–549.

Gibson, R.A., Sherry, A., Kaur, G., Pancost, R.D., Talbot, H.M., 2014. Bacteriohopanepolyols preserved in silica sinters from Champagne Pool (New Zealand) indicate a declining temperature gradient over the lifetime of the vent. Org. Geochem. 69, 61–69. https://doi.org/https://doi.org/10.1016/j.orggeochem.2014.02.004

Goesmann, F., Brinckerhoff, W.B., Raulin, F., Goetz, W., Danell, R., Getty, S., Siljeström, S., Steininger, H., Arevalo Jr., R., Buch, A., Freissinet, C., Grubisi, A., Meierhenrich, U., Mißbach, H., Pinnick, V., Stalport, F., Szopa, C., Brucato, J.R., Glavin, D.P., Grand, N., Li, X., van Amerom, F.H.W., the MOMA Science Team, 2017. The Mars Organic Molecule Analyzer (MOMA) Instrument: Characterization of Organic Material in Martian Sediments. Astrobiology 17, 655–685. https://doi.org/10.1089/ast.2016.1551

Goetz, W., Brinckerhoff, W.B., Arevalo, R., Freissinet, C., Getty, S., Glavin, D.P., Siljeström, S., Buch, A., Stalport, F., Grubisic, A., Li, X., Pinnick, V., Danell, R., van Amerom, F.H.W., Goesmann, F., Steininger, H., Grand, N., Raulin, F., Szopa, C., Meierhenrich, U., Brucato, J.R., 2016. MOMA: the challenge to search for organics and biosignatures on Mars. Int. J. Astrobiol. 15, 239–250. https://doi.org/DOI: 10.1017/S1473550416000227

Grasset, L., Guignard, C., Amblès, A., 2002. Free and esterified aliphatic carboxylic acids in

Mary Ann Liebert, Inc., 140 Huguenot Street, New Rochelle, NY 10801

humin and humic acids from a peat sample as revealed by pyrolysis with tetramethylammonium hydroxide or tetraethylammonium acetate. Org. Geochem. 33, 181–188. https://doi.org/http://dx.doi.org/10.1016/S0146-6380(01)00150-4

Grimalt, J., Albaiges, J., 1987. Sources and occurrence of C12 to C22n-alkane distributions with even carbon-number preference in sedimentary environments. Geochim. Cosmochim. Acta 51, 1379–1384.

Guido, D.M., Channing, A., Campbell, K.A., Zamuner, A., 2010. Jurassic geothermal landscapes and fossil ecosystems at San Agustín, Patagonia, Argentina. J. Geol. Soc. London. 167, 11–20.

Guignard, C., Lemee, L., Ambles, A., 2005. Lipid constituents of peat humic acids and humin. Distinction from directly extractable bitumen components using TMAH and TEAAc thermochemolysis. Org. Geochem. 36, 287–297.

Hays, L.E., Achenbach, L.A., Bailey, J., Barnes, R., Baross, J., Bertka, C., Boston, P.J., Boyd, E.S., Cable, M., Chen, I., Ciesla, F., Des Marais, D.J., Domagal-Goldman, S.D., Cook, J.E., Goldman, A., Hud, N., Laine, P., Lloyd, K., Lyons, T.W., Meadows, V.S., Mix, L.J., Mojzsis, S.J., Muller, S., Pasek, M., Powell, M., Robinson, T., Rosenzweig, F., Schmidt, B., Seelig, B., Springsteen, G., Vance, S., Welander, P., Williams, L., Wordsworth, R., 2015. NASA Astrobiology Strategy 2015.

Hays, L.E.L.E., Graham, H.V.H.V., Des Marais, D.J.D.J., Hausrath, E.M.E.M., Horgan, B., McCollom, T.M.T.M., Parenteau, M.N.N., Potter-McIntyre, S.L., Williams, A.J.A.J., Lynch, K.L.K.L., 2017. Biosignature Preservation and Detection in Mars Analog Environments. Astrobiology 17, 363–400. https://doi.org/10.1089/ast.2016.1627

He, Y., Buch, A., Morisson, M., Szopa, C., Freissinet, C., Williams, A.J., Millan, M., Guzman, M., Gonzalez, R.N., Bonnet, J.Y., Coscia, D., Mahaffy, P., Johnson, S.S., 2019. Application of TMAH thermochemolysis to the detection of nucleobases: application to the MOMA and SAM space experiment. Talanta submitted.

Herdianita, N.R., Browne, P.R.L., Rodgers, K.A., Campbell, K.A., 2000. Mineralogical and textural changes accompanying ageing of silica sinter. Miner. Depos. 35, 48–62.

https://doi.org/10.1007/s001260050005

Jahnke, L.L., Eder, W., Huber, R., Hope, J.M., Hinrichs, K.U., Hayes, J.M., Des Marais, D.J., Cady, S.L., Summons, R.E., 2001. Signature lipids and stable carbon isotope analyses of Octopus Spring hyperthermophilic communities compared with those of Aquificales representatives. Appl. Environ. Microbiol. 67, 5179–5189. https://doi.org/10.1128/AEM.67.11.5179-5189.2001

Johnson, S.S., Millan, M., Graham, H., Benison, K.C., Williams, A.J., Mcadam, A., Knudson, C.A., Andrejkovic, S., Achilles, C.N., 2020. Lipid Biomarkers in Ephemeral Acid Salt Lake Mudflat/Sandflat Sediments: Implications for Mars. Astrobiology 20, 167–178. https://doi.org/10.1089/ast.2017.1812

Jones, B., Renaut, R.W., 1996. Influence of thermophilic bacteria on calcite and silica precipitation in hot springs with water temperatures above 90 °C: evidence from Kenya and New Zealand. Can. J. Earth Sci. 33, 72–83. https://doi.org/10.1139/e96-008

Jones, B., Renaut, R.W., Rosen, M.R., 2000. Stromatolites Forming in Acidic Hot-Spring Waters, North Island, New Zealand. Palaios 15, 450–475. https://doi.org/10.1669/0883-1351(2000)015<0450:SFIAHS>2.0.CO;2

Jones, B., Renaut, R.W., Rosen, M.R., 1997. Biogenicity of silica precipitation around geysers and hot-spring vents, North Island, New Zealand. J. Sediment. Res. 67, 88–104.

Kashefi, K., Lovley, D.R., 2003. Extending the Upper Temperature Limit for Life. Science (80-.). 301, 934 LP – 934. https://doi.org/10.1126/science.1086823

Kaur, G., Mountain, B.W., Hopmans, E.C., Pancost, R.D., 2011. Preservation of Microbial Lipids in Geothermal Sinters. Astrobiology 11, 259–274. https://doi.org/10.1089/ast.2010.0540

Kaur, G., Mountain, B.W., Pancost, R.D., 2008. Microbial membrane lipids in active and inactive sinters from Champagne Pool, New Zealand: Elucidating past geothermal chemistry and microbiology. Org. Geochem. 39, 1024–1028. https://doi.org/https://doi.org/10.1016/j.orggeochem.2008.04.016

Kaur, G., Mountain, B.W., Stott, M.B., Hopmans, E.C., Pancost, R.D., 2015. Temperature and

Mary Ann Liebert, Inc., 140 Huguenot Street, New Rochelle, NY 10801

pH control on lipid composition of silica sinters from diverse hot springs in the Taupo Volcanic Zone, New Zealand. Extremophiles 19, 327–344. https://doi.org/10.1007/s00792-014-0719-9

Killops, S., Killops, V., 2005. Introduction to Organic Geochemistry, 2nd ed. Blackwell Publishing.

Konhauser, K.O., Phoenix, V.R., Bottrell, S.H., Adams, D.G., Head, I.M., 2001. Microbial–silica interactions in Icelandic hot spring sinter: possible analogues for some Precambrian siliceous stromatolites. Sedimentology 48, 415–433. https://doi.org/10.1046/j.1365-3091.2001.00372.x

Larter, S.R., Horsfield, B., 1993. Determination of structural components of kerogens by the use of analytical pyrolysis methods, in: Engel, M.H., Macko, S.A. (Eds.), Organic Geochemistry. Plenum Press, pp. 271–288.

Leira, M., Meijide-Failde, R., Torres, E., 2017. Diatom communities in thermo-mineral springs of Galicia (NW Spain). Diatom Res. 32, 29–42. https://doi.org/10.1080/0269249X.2017.1286266

Mahaffy, P.R., Webster, C.R., Cabane, M., Conrad, P.G., Coll, P., Atreya, S.K., Arvey, R., Barciniak, M., Benna, M., Bleacher, L., Brinckerhoff, W.B., Eigenbrode, J.L., Carignan, D., Cascia, M., Chalmers, R.A., Dworkin, J.P., Errigo, T., Everson, P., Franz, H., Farley, R., Feng, S., Frazier, G., Freissinet, C., Glavin, D.P., Harpold, D.N., Hawk, D., Holmes, V., Johnson, C.S., Jones, A., Jordan, P., Kellogg, J., Lewis, J., Lyness, E., Malespin, C.A., Martin, D.K., Maurer, J., McAdam, A.C., Mclennan, D., Nolan, T.J., Noriega, M., Pavlov, A.A., Prats, B., Raaen, E., Sheinman, O., Sheppard, D., Smith, J., Stern, J.C., Tan, F., Trainer, M., Ming, D.W., Morris, R. V, Jones, J., Gundersen, C., Steele, A., Wray, J., Botta, O., Leshin, L.A., Owen, T., Battel, S., Jakosky, B.M., Manning, H., Squyres, S., Christopher, R.N., Francois, P.M., Sternberg, R., Buch, A., Sorensen, P., Coscia, D., Szopa, C., Teinturier, S., Baffes, C., Feldman, J., Flesch, G., Forouhar, S., Garcia, R., Keymeulen, D., Woodward, S., Block, B.P., Arnett, K., Miller, R., Edmonson, C., Gorevan, S., 2012. The Sample Analysis at Mars Investigation and Instrument Suite. Space Sci. Rev. 1–78. https://doi.org/10.1007/s11214-012-9879-z

McCollom, T.M., Hynek, B.M., Rogers, K.L., 2016. Potential for preservation of biosignatures from endolithic microbial communities in a Mars analog fumarole environment, in: Biosignature Preservation and Detection in Mars Analog Environments. p. 2006.

McCollom, T.M., Ritter, G., Simoneit, B., 1999. Lipid Synthesis under Hydrothermal Conditions by Fischer-Tropsch-Type Reactions. Orig. Life Evol. Biosph. 29, 153–166.

Metcalffe, L.D., Wang, C.N., 1981. Rapid Preparation of Fatty Acid Methyl Esters Using Organic Base-Catalyzed Transesterification. J. Chromatogr. Sci. 19, 530–535.

Millan, M., Malespin, C.A., Freissinet, C., Glavin, D.P., Mahaffy, P.R., Buch, A., Szopa, C., Srivastava, A., Teinturier, S., Williams, R., Williams, A.J., McAdam, A., Coscia, D., Eigenbrode, J., Raaen, E., Dworkin, J., Navarro-Gonzalez, R., Johnson, S.S., 2019. Lessons learned from the full cup wet chemistry experiment performed on mars with the sample analysis at mars instrument, in: Mars 9 Conference. p. 6210.

Munoz-Saez, C., Salthiel, S., Manga, M., Nguyen, C., Gonnermann, H., 2016. Physical and hydraulic properties of modern sinter deposits: El Tatio, Atacama. J. Volcanol. Geotherm. Res. 325, 156–168.

Nishimura, M., Baker, E., 1986. Possible origin of n-alkanes with a remarkable even-to-odd predominance in recent marine sediments. Geochim. Cosmochim. Acta 50, 299–305.

O'Reilly, S.S., Mariotti, G., Winter, A.R., Newman, S.A., Matys, E.D., McDermott, F., Pruss, S.B., Bosak, T., Summons, R.E., Klepac-Ceraj, V., 2017. Molecular biosignatures reveal common benthic microbial sources of organic matter in ooids and grapestones from Pigeon Cay , The Bahamas. Geobiology 112–130. https://doi.org/10.1111/gbi.12196

Oshima, M., Miyagawa, A., 1974. Comparative studies on the fatty acid composition of moderately and extremely thermophilic bacteria. Lipids 9, 476–480. https://doi.org/10.1007/BF02534274

Pancost, R.D., Pressley, S., Coleman, J.M., Benning, L.G., Mountain, B.W., 2005. Lipid biomolecules in silica sinters: indicators of microbial biodiversity. Environ. Microbiol. 7, 66–77. https://doi.org/10.1111/j.1462-2920.2004.00686.x

Pancost, R.D., Pressley, S., Coleman, J.M., Talbot, H.M., Kelly, S.P., Farrimond, P., Schouten,

S., Benning, L., Mountain, B.W., 2006. Composition and implications of diverse lipids in New Zealand Geothermal sinters. Geobiology 4, 71–92. https://doi.org/10.1111/j.1472-4669.2006.00069.x

Pavlov, A.A., Vasilyev, G., Ostryakov, V.M., Pavlov, A.K., Mahaffy, P., 2012. Degradation of the organic molecules in the shallow subsurface of Mars due to irradiation by cosmic rays. Geophys. Res. Lett. 39. https://doi.org/10.1029/2012GL052166

Pulchan, J., Abrajano, T.A., Helleur, R., 1997. Characterization of tetramethylammonium hydroxide thermochemolysis products of near-shore marine sediments using gas chromatography/mass spectrometry and gas chromatography/combustion/isotope ratio mass spectrometry. J. Anal. Appl. Pyrolysis 42, 135–150.

Pumas, C., Pruetiworanan, S., Peerapornpisal, Y., 2018. Diatom diversity in some hot springs of northern Thailand. Botanica 24, 69–86. https://doi.org/https://doi.org/10.2478/botlit-2018-0007

Ray, P.H., White, D.C., Brock, T.D., 1971. Effect of temperature on the fatty acid composition of Thermus aquaticus. J. Bacteriol. 106, 25–30.

Renaut, R.W., Jones, B., 2011. Hydrothermal environments, terrestrial, in: Reitner, J., Thiel, V. (Eds.), Encyclopedia of Geobiology. Springer, pp. 467–479.

Renaut, R.W., Jones, B., Tiercelin, J.J., 1998. Rapid in situ silicification of microbes at Loburu hot springs, Lake Bogoria, Kenya rift valley. Sedimentology 45, 1083–1103. https://doi.org/10.1046/j.1365-3091.1998.00194.x

Rossi, A.P., Neukum, G., Pondrelli, M., van Gasselt, S., Zegers, T., Hauber, E., Chicarro, A., Foing, B., 2008. Large-scale spring deposits on Mars? J. Geophys. Res. E Planets 113, 1–17. https://doi.org/10.1029/2007JE003062

Ruff, S.W., Farmer, J.D., 2016. Silica deposits on Mars with features resembling hot spring biosignatures at El Tatio in Chile. Nat. Commun. 7, 13554.

Ruff, S.W., Farmer, J.D., Calvin, W.M., Herkenhoff, K.E., Johnson, J.R., Morris, R. V, Rice, M.S., Arvidson, R.E., Bell III, J.F., Christensen, P.R., Squyres, S.W., 2011. Characteristics, distribution, origin, and significance of opaline silica observed by the Spirit rover in Gusev

crater, Mars. J. Geophys. Res. E Planets 116. https://doi.org/10.1029/2010JE003767

Russell, N.J., 1984. Mechanisms of thermal adaptation in bacteria: blueprints for survival. Trends Biochem. Sci. 9, 108–112. https://doi.org/https://doi.org/10.1016/0968-0004(84)90106-3

Saini, J., Kaur, R., Sharma, P.K., 2017. Metagenomic Insights into Microbial Diversity and Metabolic Potential of Hot Spring Ecosystems BT - Mining of Microbial Wealth and MetaGenomics, in: Kalia, V.C., Shouche, Y., Purohit, H.J., Rahi, P. (Eds.), . Springer Singapore, Singapore, pp. 143–159. https://doi.org/10.1007/978-981-10-5708-3_9

Schulten, H.R., 1996. Direct pyrolysis-mass spectrometry of soils: a novel tool in agriculture, ecology, forestry and soil science, in: Yamasaki, S., Boutton, T.W. (Eds.), Mass Spectrometry of Soils. Marcel Dekker, New York, pp. 373–436.

Segerer, A.H., Burggraf, S., Fiala, G., Huber, G., Huber, R., Pley, U., Stetter, K.O., 1993. Life in hot springs and hydrothermal vents. Orig. Life Evol. Biosph. 23, 77–90.

Shen, P.Y., Coles, E., Foote, J.L., Stenesh, J., 1970. Fatty Acid Distribution in Mesophilic and Thermophilic Strains of the Genus Bacillus J. Bacteriol. 103, 479 LP – 481.

Shiea, J., Brassel, S.C., Ward, D.M., 1991. Comparative analysis of extractable lipids in hot spring microbial mats and their component photosynthetic bacteria. Org. Geochem. 17, 309–319. https://doi.org/https://doi.org/10.1016/0146-6380(91)90094-Z

Skirnisdottir, S., Hreggvidsson, G.O., Hjörleifsdottir, S., Marteinsson, V.T., Petursdottir, S.K., Holst, O., Kristjansson, J.K., 2000. Influence of Sulfide and Temperature on Species Composition and Community Structure of Hot Spring Microbial Mats. Appl. Environ. Microbiol. 66, 2835 LP – 2841. https://doi.org/10.1128/AEM.66.7.2835-2841.2000

Skok, J.R., Mustard, J.F., Ehlmann, B.L., Milliken, R.E., Murchie, S.L., 2010. Silica deposits in the Nili Patera caldera on the Syrtis Major volcanic complex on Mars. Nat. Geosci. 3, 838–841.

Squyres, S.W., Arvidson, R.E., Ruff, S., Gellert, R., Morris, V., Ming, D.W., Crumpler, L., Farmer, J.D., Marais, D.J. Des, Yen, A., McLennan, S.M., Calvin, W., Bell, J.F., B. C.

Clark, 11 A. Wang, 2 T. J. McCoy, 12 M. E. Schmidt, 12 P. A. de Souza Jr.13, 2008. Detection of Silica-Rich Deposits on Mars. Science (80-.). 320, 1063–1067. https://doi.org/10.1126/science.1155429

Summons, R.E., Albrecht, P., Mcdonald, G., Moldowan, J.M., 2008. Molecular Biosignatures. Space Sci. Rev. 135, 133–159. https://doi.org/10.1007/s11214-007-9256-5

Summons, R.E., Bird, L.R., Gillespie, A.L., Pruss, S.B., Roberts, M., Sessions, A.L., 2013. Lipid biomarkers in ooids from different locations and ages: evidence for a common bacterial flora. Geobiology 11, 420–436. https://doi.org/10.1111/gbi.12047

Sun, M.-Y., Wakeham, S., Lee, C., 1997. Rates and mechanisms of fatty acid degradation in oxic and anoxic coastal marine sediments of Long Island Sound, New York, USA. Geochim. Cosmochim. Acta1 61, 341–355.

Tarhan, L.G., Hood, A. v. S., Droser, M.L., Gehling, J.G., Briggs, D.E.G., 2016. Exceptional preservation of soft-bodied Ediacara Biota promoted by silica-rich oceans. Geology 44, 951–954. https://doi.org/10.1130/G38542.1

Teece, B.L., George, S.C., Djokic, T., Campbell, K.A., Ruff, S.W., Kranendonk, M.J. Van, 2020. Biomolecules from fossilized hot-spring sinters: implications for the search for life on Mars. Astrobiology 20, 537–551.

Vestal, J.R., White, D.C., 1989. Lipid Analysis in Microbial Ecology. Bioscience 39, 535–541.

Volkman, J., 2006. Lipid biomarkers for marine organic matter, in: Volkman, J. (Ed.), Marine Organic Matter: Biomarkers, Isotopes and DNA. Heidelberg: Springer-Verlag, Berlin, pp. 27–70.

Volkman, J., Jeffrey, S., Nichols, P., Rogers, G., Farland, C., 1989. Fatty acid and lipid composition of 10 species of microalgae used in mariculture. J. Exp. Mar. Bio. Ecol. 128.

Walter, M.R., 1996. Ancient hydrothermal ecosystems on earth: a new palaeobiological frontier, in: Ciba Foundation Symposium. pp. 112–127 (discussion 127–130).

Walter, M.R., 1976. Hot-spring sediments in Yellowstone National Park, in: Walter, M.R. (Ed.), Stromatolites. Elsevier, Amsterdam, pp. 489–198.

Walter, M.R., Des Marais, D.J., 1993. Preservation of Biological Information in Thermal Spring Deposits: Developing a Strategy for the Search for Fossil Life on Mars. Icarus 101, 129–143.

Ward, D.M., Castenholz, R.W., Miller, S.R., 2012. Cyanobacteria in Geothermal Habitats, in: Whitton, B.A. (Ed.), Ecology of Cyanobacteria II: Their Diversity in Space and Time. Springer, pp. 39–63. https://doi.org/10.1007/978-94-007-3855-3_3

Weerkamp, A., Heinen, W., 1972. Effect of temperature on the fatty acid composition of the extreme thermophiles, Bacillus caldolyticus and Bacillus caldotenax. J. Bacteriol. 109, 443–446.

Westall, F., Campbell, K.A., Bréhéret, J.G., Foucher, F., Gautret, P., Hubert, A., Sorieul, S., Grassineau, N., Guido, D.M., 2015. Archean (3.33 Ga) microbe-sediment systems were diverse and flourished in a hydrothermal context. Geology 43, 615–618. https://doi.org/10.1130/G36646.1

Wilhelm, M.B., Davila, A.F., Eigenbrode, J.L., Parenteau, M.N., Jahnke, L.L., Liu, X., Summons, R.E., Wray, J.J., Stamos, B.N., O'Reilly, S.S., Williams, A.J., 2017. Xeropreservation of functionalized lipid biomarkers in hyperarid soils in the Atacama Desert. Org. Geochem. 103, 97–104. https://doi.org/10.1016/j.orggeochem.2016.10.015

Williams, A.J., Eigenbrode, J., Floyd, M., Wilhelm, M.B., O'Reilly, S., Johnson, S.S., Craft, K.L., Knudson, C.A., Andrejkovičová, S., Lewis, J.M.T., Buch, A., Glavin, D.P., Freissinet, C., Williams, R.H., Szopa, C., Millan, M., Summons, R.E., McAdam, A., Benison, K., Navarro-González, R., Malespin, C., Mahaffy, P.R., 2019. Recovery of Fatty Acids from Mineralogic Mars Analogs by TMAH Thermochemolysis for the Sample Analysis at Mars Wet Chemistry Experiment on the Curiosity Rover. Astrobiology 19, 522–546. https://doi.org/10.1089/ast.2018.1819

Zhang, C.L., Fouke, B.W., Bonheyo, G.T., Peacock, A.D., White, D.C., Huang, Y., Romanek, C.S., 2004. Lipid biomarkers and carbon-isotopes of modern travertine deposits (Yellowstone National Park, USA): Implications for biogeochemical dynamics in hot-spring systems. Geochim. Cosmochim. Acta 68, 3157–3169. https://doi.org/https://doi.org/10.1016/j.gca.2004.03.005

Zhang, C.L., Huang, Z., Li, Y.-L., Romanek, C.S., Mills, G.L., Gibson, R.A., Talbot, H.M., Wiegel, J., Noakes, J., Culp, R., White, D.C., 2007. Lipid Biomarkers, Carbon Isotopes, and Phylogenetic Characterization of Bacteria in California and Nevada Hot Springs. Geomicrobiol. J. 24, 519–534. https://doi.org/10.1080/01490450701572515

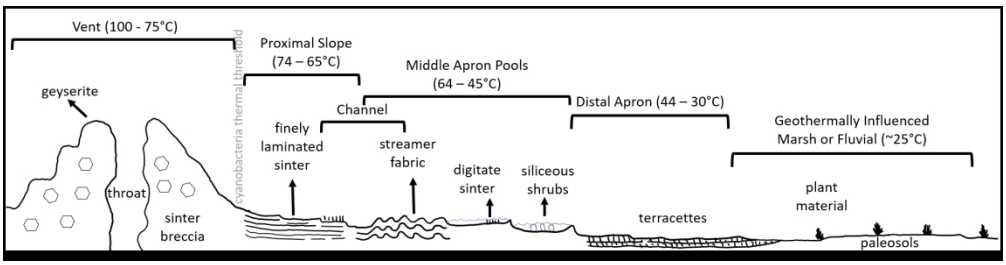

Figure 1. Environmental settings and facies of a generalized geothermal spring system. Modified from Campbell et al. (2015).

321x81mm (150 x 150 DPI)

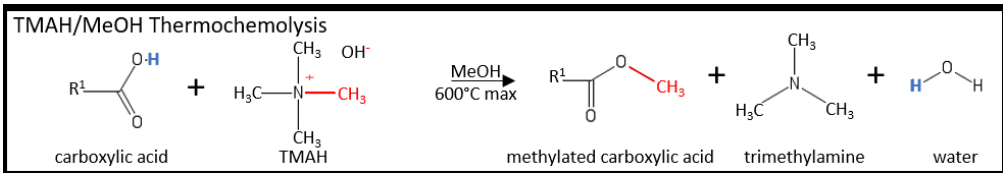

Figure 2. Example TMAH thermochemolysis reaction with a carboxylic acid to form a methylated carboxylic acid. After the reaction, the molecule is more volatile and detectable to GC-MS. TMAH in methanol is available on the SAM and MOMA instruments.

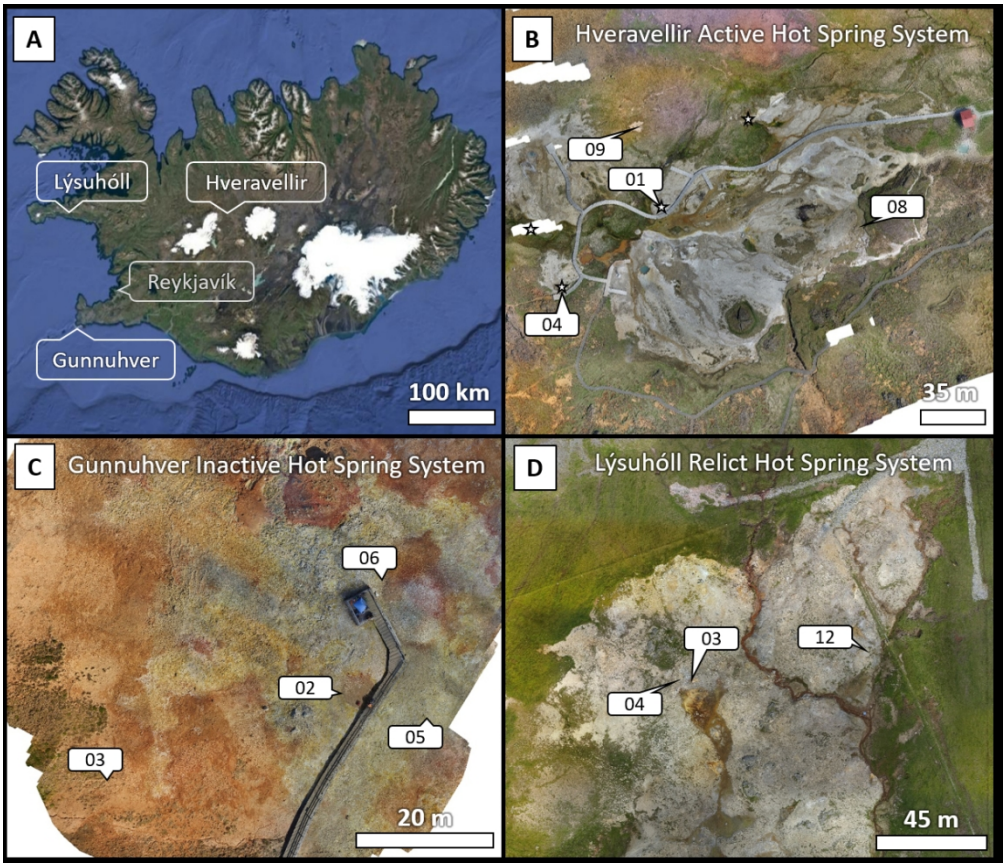

Figure 3. A) Map of field locations in Iceland, with the capitol of Reykjavík for reference. B-D) Field site numbers at the Hveravellir, Gunnuhver, and Lýsuhóll spring systems. Stars at Hveravellir indicate active flowing spring vents where geochemical measurements were taken.

209x180mm (150 x 150 DPI)

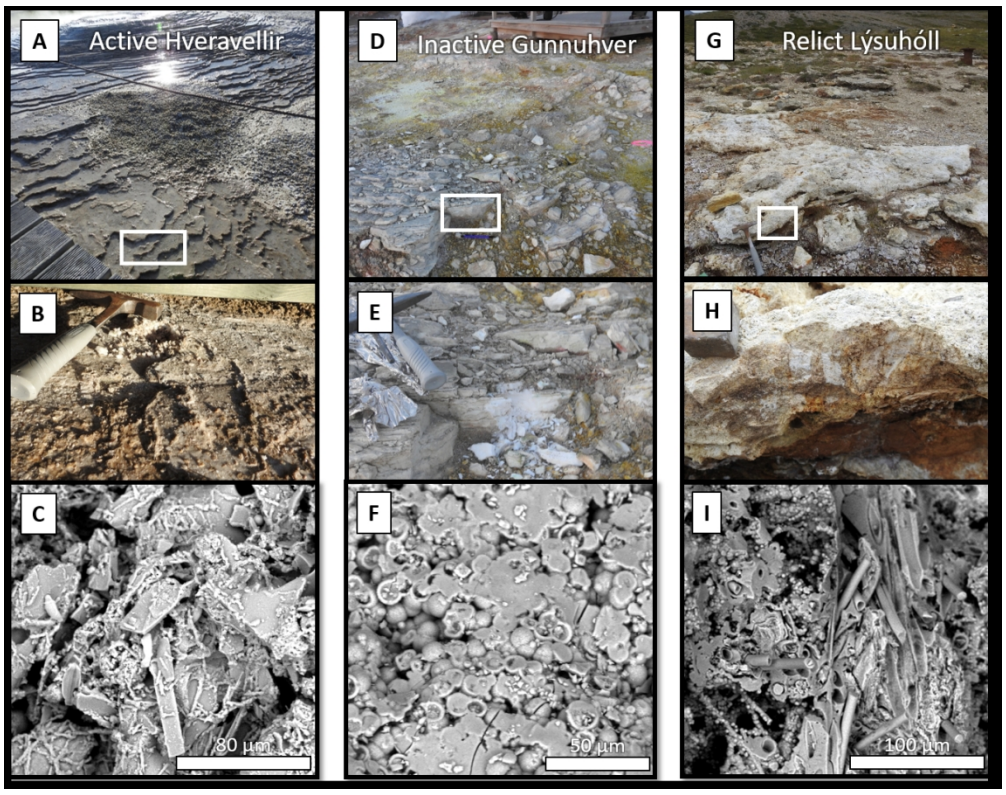

Figure 4. Field sample site images and corresponding SEM images of sinter from A-C) Hveravellir (active vent in top left of panel A), D-F) Gunnuhver, and G-I) Lýsuhóll. White box indicates zoom image B, E, or H. Rock hammer for scale in surface images. C) Silificied diatoms, microbial filaments, and putative plant matter present in the Hveravellir site. F) Opal-CT accretionary spheres with no confirmed biogenic features present in the Gunnuhver site. I) Abundant silicified casts of microbial filaments present in the Lýsuhóll site.

229x179mm (150 x 150 DPI)

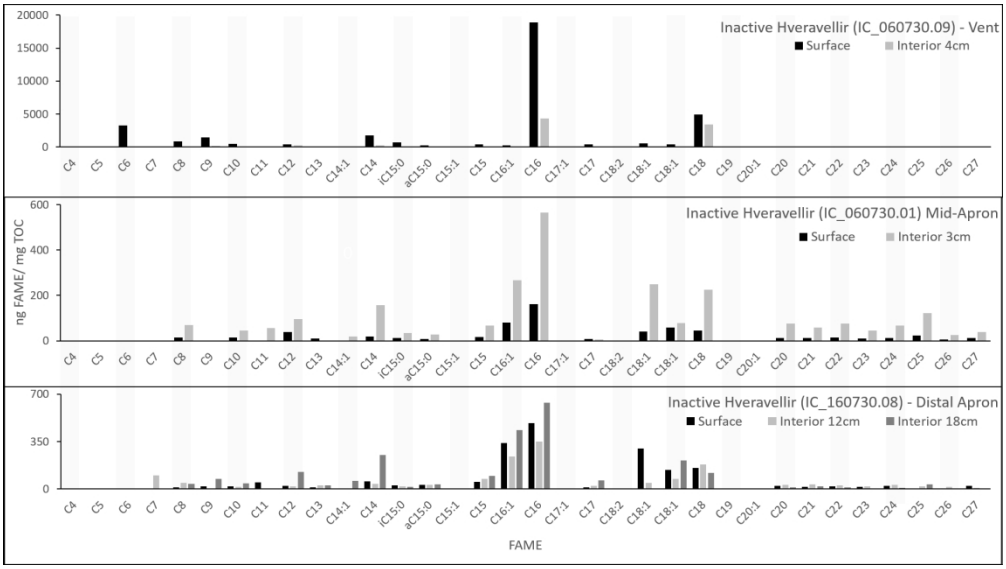

Figure 5. FAME profile for the active Hveravellir Hot Spring system analyzed with a 500 °C flash pyrolysis step.

339x190mm (150 x 150 DPI)

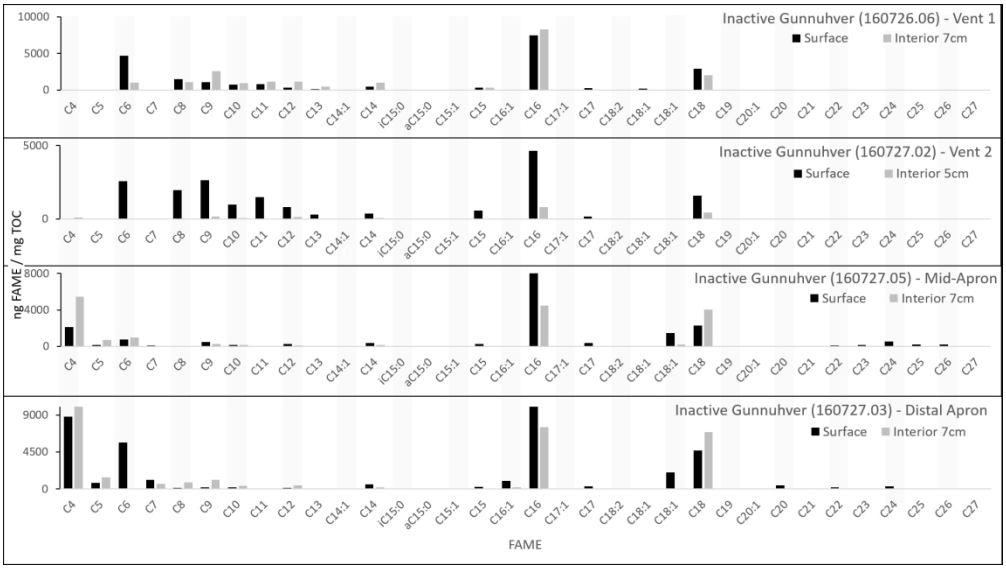

Figure 6. FAME profile for the inactive Gunnuhver Hot Spring system analyzed with a 500 °C flash pyrolysis step.

339x190mm (150 x 150 DPI)

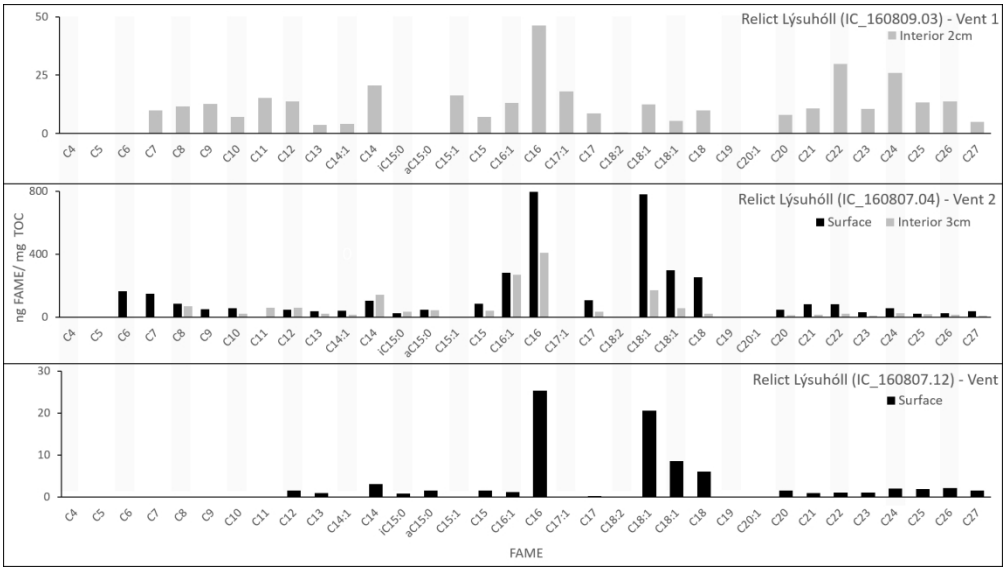

Figure 7. FAME profile for the relict Lýsuhóll Hot Spring system analyzed with a 500 °C flash pyrolysis step.

339x190mm (150 x 150 DPI)

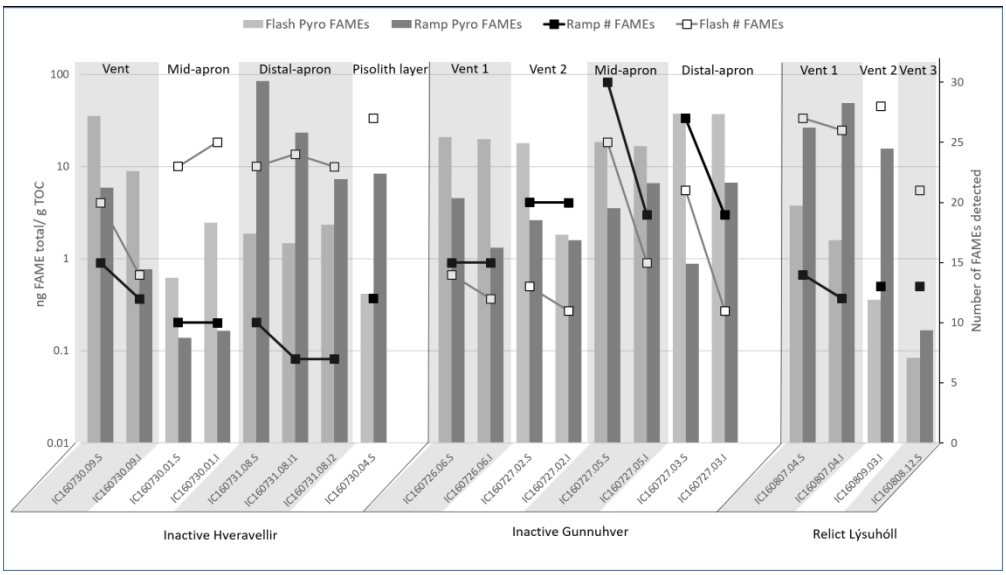

Figure 8. Comparison of total FAME abundance (in ng FAME/ g TOC) detected with the 500°C flash pyrolysis and the SAM-like 35°C/min ramp pyrolysis methods at each sinter sample location. The number of unique FAMEs detected with each pyrolysis method is included on the secondary (right) y-axis. Flash pyrolysis nearly always yielded comparable numbers of FAMEs relative to ramp pyrolysis.

339x191mm (150 x 150 DPI)

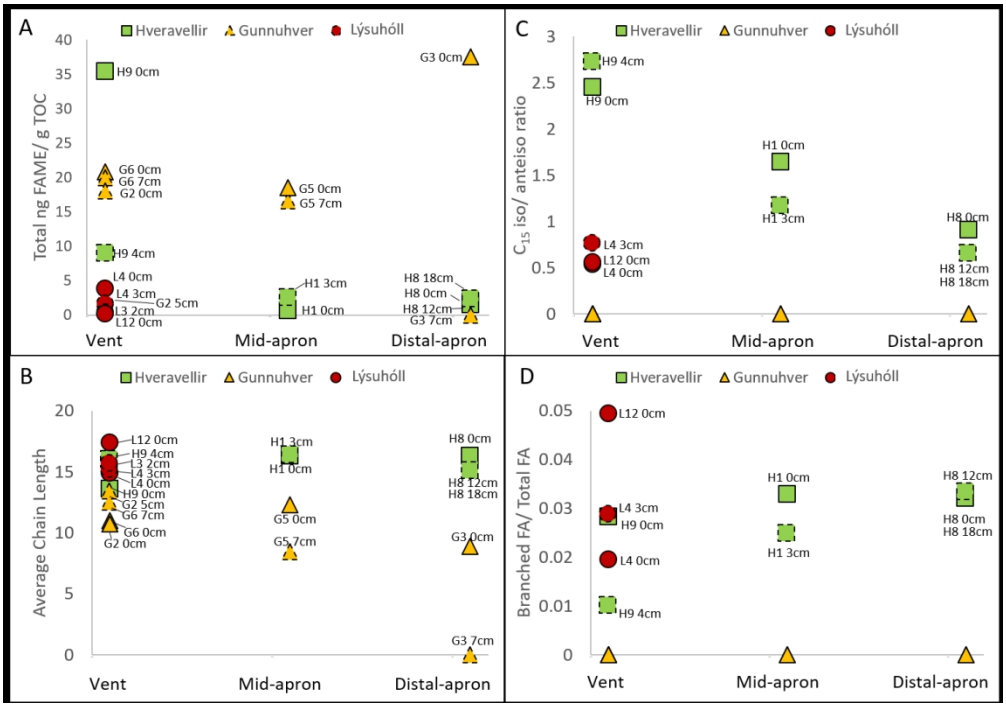

Figure 9. Fatty acid distribution across hot spring facies, with locations "vent", "mid-apron" and "distal-apron" representing environmental facies as determined by textural characterization. A) Total ng of FAMEs / g TOC. The total FAME concentration at the Hveravellir site is highest at the vent, whereas the concentration at the Gunnuhver site is highest at the distal apron. B) The average carbon chain length at the Hveravellir site slightly increases from vent to distal apron, whereas at the Gunnuhver site the average chain length dramatically decreases. C) The ratio of iso- to anteiso-C15 is highest in the Hveravellir vent site and lowest in the distal apron facies. No br-FA were detected in the Gunnuhver site. The br-FA ratio was low for the Lýsuhóll vent sites. D) The ratio of branched fatty acids to total fatty acids was lowest at the Hveravellir vent site and highest at the distal apron site. No br-FA were detected in the Gunnuhver site. The ratio of br-FA to total FA was higher for the Lýsuhóll vent sites.

256x179mm (150 x 150 DPI)

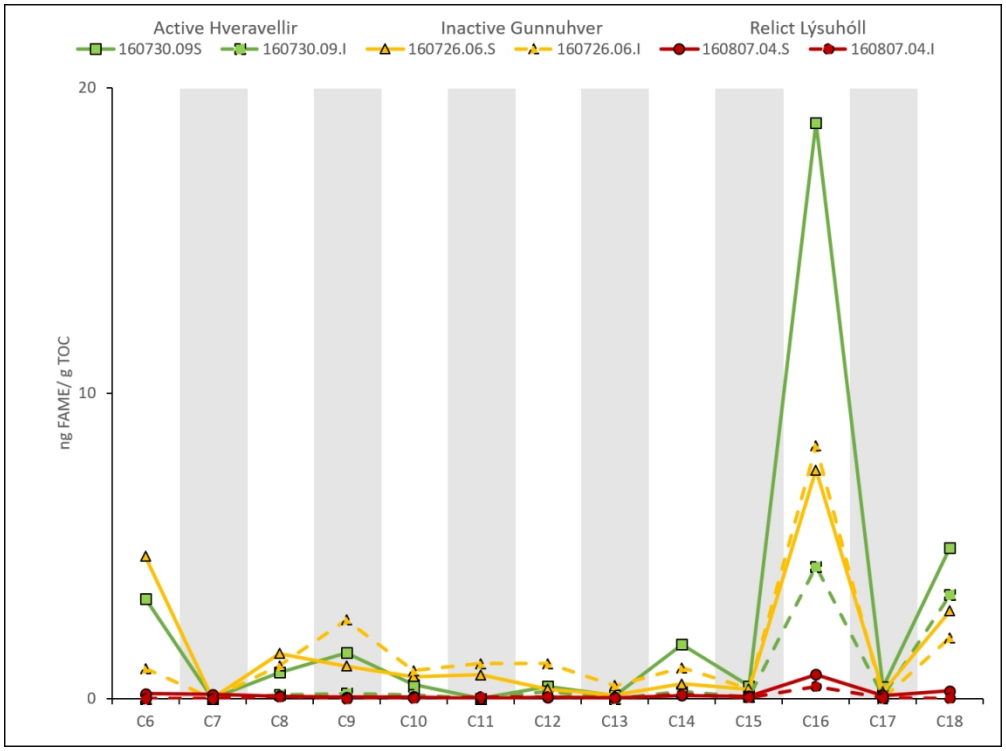

Figure 10. Comparison of FAME concentrations determined with flash pyrolysis experiments from the surface and subsurface vent sites from the Hveravellir, Gunnuhver, and Lýsuhóll spring systems. The even-over-odd carbon number preference is most apparent in the Hveravellir and Gunnuhver locations.

242x180mm (150 x 150 DPI)

Table 1. Sample location, ID, depth, mineralogy, latitude, longitude, percent total carbon and percent total organic carbon.								
Group	*Sample ID*	*Sample*	*Sample Depth*	*Mineralogy*	*Latitude*	*Longitude*	*% TC*	*% TOC ±0.06*
Hveravellir Modern Active Spring System	IC160730.09.S	Vent deposit	0 cm	Opal-A, clinopyroxenes (e.g. augite, diopside), plagioclase, gypsum	N64° 51.940’	W19° 33.513’	0.24	0.24
	IC160730.09.I	Vent deposit	4 cm	Opal-A, plagioclase, diopside, magnesite			0.08	0.08
	IC160730.01.S	Mid-apron deposit	0 cm	Amorphous	N64° 51.917’	W19° 33.437’	0.43	0.43
	IC160730.01.I	Mid-apron deposit	3 cm	Amorphous			0.10	0.10
	IC160731.08.S	Distal apron deposit	0 cm	Amorphous	N64° 51.911’	W19° 33.363’	0.08	0.08
	IC160731.08.I1	Distal apron deposit	12 cm	Amorphous			0.13	0.13
	IC160731.08.I2	Distal apron deposit	18 cm	Amorphous			0.15	0.15
	IC160730.04.S	Pisolith layer	0 cm	Opal-A, plagioclase, magnesite	N64° 51.893’	W19° 33.564’	0.30	0.30
Gunnuhver Modern Inactive Spring System	IC160726.06.S	Vent deposit	0 cm	Opal-CT	N63° 49.148’	W022° 41.159’	0.02	0.02
	IC160726.06.I	Vent deposit	7 cm	Opal-CT			0.01	0.01
	IC160727.02.S	Vent deposit	0 cm	Opal-CT, halite, quartz	N63° 49.138’	W022° 41.168’	0.13	0.13
	IC160727.02.I	Vent deposit	5 cm	Opal-CT, halite, quartz			0.02	0.02
	IC160727.05.S	Mid-apron deposit	0 cm	Opal-CT	N63° 49.136’	W022° 41.149’	0.17	0.17
	IC160727.05.I	Mid-apron deposit	7 cm	Opal-CT			0.02	0.02
	IC160727.03.S	Distal apron deposit	0 cm	Amorphous	N63° 49.131’	W022° 41.205’	0.15	0.15
	IC160727.03.I	Distal apron deposit	7 cm	Amorphous			0.02	0.02
Lýsuhóll Relict Spring System	IC160807.04.S	Vent deposit	0 cm	Amorphous, calcite	N64° 50.651’	W023° 13.281’	1.83	0.61
	IC160807.04.I	Vent deposit	3 cm	Amorphous, calcite			0.85	0.18
	IC160809.03.I	Vent deposit	2 cm	Amorphous, minor calcite	N64° 50.650’	W023° 13.274’	0.61	0.43
	IC160808.12.S	Vent deposit	0 cm	Calcite	N64° 50.657’	W023° 13.177’	10.38	6.31

Table 1. Sample location, ID, depth, mineralogy, latitude, longitude, percent total carbon and percent total organic carbon.

Table 2. Flash pyrolysis FAME data in ng FAME/ mg TOC.

Group	*Sample ID*	C4	C5	C6	C7	C8	C9	C10	C11	C12	C13	C14:1	C14	iC15:0	aC15:0	C15:1	C15
Hveravellir Modern Active Spring System	IC160730.09.S	0.0	0.0	3281.4	0.0	862.1	1501.0	467.5	0.0	400.4	110.5	0.0	1780.5	711.3	290.4	0.0	419.3
	IC160730.09.I	0.0	0.0	0.0	0.0	136.2	171.8	127.7	0.0	247.3	0.0	0.0	231.9	66.4	24.4	0.0	68.2
	IC160730.01.S	0.0	0.0	0.0	0.0	13.8	0.0	13.9	0.0	38.9	9.2	0.0	19.5	12.8	7.8	0.0	17.3
	IC160730.01.I	0.0	0.0	0.0	0.0	68.5	0.0	45.0	57.0	95.0	1.6	18.5	157.3	33.1	28.2	0.0	67.4
	IC160731.08.S	0.0	0.0	0.0	0.0	11.0	18.5	18.4	49.8	22.3	14.1	0.0	57.2	28.5	31.4	0.0	53.2
	IC160731.08.I1	0.0	0.0	0.0	100.0	47.0	0.0	16.9	0.0	19.6	26.7	0.0	37.6	19.4	29.7	0.0	75.0
	IC160731.08.I2	0.0	0.0	0.0	0.0	38.7	74.3	41.1	0.0	126.4	25.5	61.8	252.4	14.7	36.0	0.0	98.5
Gunnuhver Modern Inactive Spring System	IC160726.06.S	0.0	0.0	4663.7	0.0	1478.2	1070.1	731.4	788.8	319.7	118.2	0.0	485.3	0.0	0.0	0.0	313.2
	IC160726.06.I	0.0	0.0	990.0	0.0	1085.4	2578.5	925.8	1147.4	1148.3	432.7	0.0	1017.4	0.0	0.0	0.0	329.4
	IC160727.02.S	0.0	0.0	2558.7	0.0	1960.6	2630.9	976.6	1494.4	807.0	310.5	0.0	377.5	0.0	0.0	0.0	554.9
	IC160727.02.I	94.7	0.0	0.0	0.0	0.0	163.1	72.9	0.0	120.3	14.8	0.0	59.1	0.0	0.0	0.0	18.9
	IC160727.05.S	2146.2	165.5	770.5	129.1	14.1	467.1	149.3	0.0	247.1	11.8	0.0	387.7	0.0	0.0	0.0	287.5
	IC160727.05.I	5466.7	683.5	1007.4	0.0	0.0	246.3	139.1	52.6	104.9	0.0	0.0	149.8	0.0	0.0	0.0	27.0
	IC160727.03.S	8777.9	715.6	5654.0	1077.1	141.7	181.6	188.0	0.0	123.7	0.0	0.0	554.0	0.0	0.0	0.0	282.1
	IC160727.03.I	17486.5	1401.0	0.0	**604.7**	**794.8**	1075.5	366.6	0.0	440.7	0.0	0.0	219.2	0.0	0.0	0.0	0.0
Lýsuhóll Relict Spring System	IC160807.04.S	0.0	0.0	163.4	147.0	84.3	49.0	57.3	0.0	46.9	36.8	39.7	104.8	25.8	48.0	0.0	83.2
	IC160807.04.I	0.0	0.0	0.0	0.0	69.1	0.0	22.3	60.2	58.6	21.8	13.7	142.7	33.8	44.4	0.0	39.5
	IC160809.03.I	0.0	0.0	0.0	9.9	11.5	12.6	7.2	15.3	13.7	3.8	4.0	20.5	0.0	0.0	16.3	7.1
	IC160808.12.S	0.0	0.0	0.0	0.0	0.0	0.0	0.0	0.0	1.6	1.0	0.0	3.1	0.9	1.5	0.0	1.5

Table 2 con't. Flash pyrolysis FAME data in ng FAME/ mg TOC.

Group	*Sample ID*	C16:1	C16	C17:1	C17	trans-C18:2	cis-C18:1	trans-C18:1	C18	C20	C21	C22	C23	C24	C25	C26	C27
Hveravellir Modern Active Spring System	IC160730.09.S	244.0	18860.8	5.5	383.7	0.0	580.2	406.4	4953.4	133.6	0.0	10.5	0.0	0.0	0.0	0.0	0.0
	IC160730.09.I	0.0	4334.5	0.0	85.0	0.0	0.0	0.0	3405.9	49.5	0.0	6.2	0.0	0.0	0.0	0.0	0.0
	IC160730.01.S	79.4	160.6	0.0	7.5	0.0	40.1	59.2	44.5	11.4	11.3	13.5	10.8	11.9	22.9	6.0	11.8
	IC160730.01.I	266.7	565.5	0.0	4.5	0.0	249.3	77.2	224.9	75.1	57.8	75.8	46.0	66.5	122.8	24.9	39.5
	IC160731.08.S	340.9	488.0	0.0	13.7	0.0	300.6	141.3	156.8	25.3	15.8	20.5	17.8	24.6	0.0	0.0	25.3
	IC160731.08.I1	239.8	351.6	0.0	22.5	0.0	47.1	73.6	180.1	29.1	35.5	26.2	21.3	29.9	18.1	17.2	9.0
	IC160731.08.I2	433.4	638.5	0.0	64.6	0.0	0.0	211.3	119.3	11.3	20.5	11.1	5.7	9.9	36.1	4.4	0.0
Gunnuhver Modern Inactive Spring System	IC160726.06.S	0.0	7484.0	0.0	237.7	0.0	165.8	0.0	2881.8	0.0	0.0	0.0	0.0	0.0	0.0	0.0	0.0
	IC160726.06.I	0.0	8282.2	0.0	0.0	0.0	0.0	0.0	1993.1	0.0	0.0	0.0	0.0	0.0	0.0	0.0	0.0
	IC160727.02.S	0.0	4655.8	0.0	152.7	0.0	0.0	0.0	1571.3	0.0	0.0	0.0	0.0	0.0	0.0	0.0	0.0
	IC160727.02.I	0.0	820.1	0.0	17.6	0.0	0.0	0.0	439.4	0.0	0.0	0.0	0.0	0.0	0.0	0.0	0.0
	IC160727.05.S	62.2	8073.3	0.0	394.7	0.0	0.0	1469.2	2295.9	76.1	16.0	110.5	143.0	556.9	216.9	212.2	18.4
	IC160727.05.I	0.0	4444.4	0.0	32.1	0.0	0.0	195.7	4021.3	0.0	0.0	0.0	0.0	0.0	0.0	0.0	0.0
	IC160727.03.S	1010.7	10647.0	0.0	296.2	0.0	0.0	1984.8	4710.6	407.2	0.0	223.2	81.4	340.7	0.0	80.4	0.0
	IC160727.03.I	181.7	7523.1	0.0	0.0	0.0	0.0	0.0	6949.7	0.0	0.0	0.0	0.0	0.0	0.0	0.0	0.0
Lýsuhóll Relict Spring System	IC160807.04.S	282.3	796.2	0.0	108.5	0.0	780.4	296.8	254.0	46.0	80.2	82.6	29.0	57.2	20.5	22.7	35.4
	IC160807.04.I	268.0	409.4	0.0	33.5	0.5	171.4	54.5	21.4	10.6	14.9	20.7	8.8	22.8	16.7	13.4	9.8
	IC160809.03.I	13.2	46.2	18.1	8.7	0.5	12.5	5.4	9.8	8.1	10.8	29.9	10.5	25.9	13.2	13.8	5.0
	IC160808.12.S	1.2	25.3	0.0	0.3	0.0	20.6	8.6	6.0	1.5	1.0	1.0	1.1	2.0	1.9	2.1	1.5

Table 2. Flash pyrolysis FAME data in ng FAME/ mg TOC. Black cells = concentrations >100 ng/ mg TOC. Dark gray cells = Concentrations 10 to 100 ng/ mg TOC. Light gray cells = 0.01 to 10 ng/ mg TOC. White cells = No detection (0.0 ng / mg TOC).

Group	Sample ID	$C_{4:0}$		$C_{5:0}$		$C_{6:0}$		$C_{7:0}$		$C_{8:0}$		$C_{9:0}$		$C_{10:0}$		$C_{11:0}$		$C_{12:0}$		$C_{13:0}$		$C_{14:1}$		$C_{14:0}$		$iC_{15:0}$		$aC_{15:0}$		$C_{15:1}$		$C_{15:0}$	
		F	R	F	R	F	R	F	R	F	R	F	R	F	R	F	R	F	R	F	R	F	R	F	R	F	R	F	R	F	R	F	R
Modern Active Spring System at Hveravellir	IC160730.09.S					x	X			x	X	x	X	x	X		X	x	X	x	X			x	X	x		x				x	X
	IC160730.09.I									x	X	x	X	x	X		X	x	X		X			x	X	x		x				x	X
	IC160730.01.S						X			x	X			x				x		x				x	X	x		x				x	X
	IC160730.01.I									x			X	x	X	x		x	X	x		x		x	X	x		x				x	X
	IC160731.08.S									x	X	x	X	x	X	x		x	X	x	X			x	X	x		x				x	X
	IC160731.08.I1							x		x				x				x	X	x	X			x	X	x		x				x	X
	IC160731.08.I2									x	X	x		x	X			x	X	x		x		x	X	x		x				x	
	IC160730.04.S					x	X			x	X	x		x	X			x	X					x	X	x		x				x	X
Modern Inactive Spring System at Gunnuhver	IC160726.06.S					x				x	X	x	X	x	X	x		x	X	x				x	X							x	X
	IC160726.06.I					x	X			x	X	x	X	x	X	x		x	X	x	X			x	X							x	X
	IC160727.02.S		X		X	x	X		X	x	X	x	X	x	X	x		x	X	x				x	X							x	X
	IC160727.02.I	x	X		X		X				X	x	X	x	X		X	x	X	x	X			x	X							x	X
	IC160727.05.S	x	X	x	X	x	X	x	X	x	X	x	X	x	X			x	X	x	X			x	X							x	X
	IC160727.05.I	x	X	x	X	x	X		X		X	x	X	x	X	x		x	X	x				x	X							x	X
	IC160727.03.S	x	X	x	X	x	X	x		x	X	x	X	x	X			x	X		X			x	X		X		X			x	X
	IC160727.03.I	x	X	x		x	X	x		x	X	x	X	x	X			x	X					x	X								X
Relict Spring System at Lýsuhóll	IC160807.04.S		X			x	X	x		x	X	x		x	X			x	X	x		x		x	X	x		x				x	X
	IC160807.04.I						X			x	X		X	x	X	x	X	x	X	x	X	x		x	X	x		x				x	X
	IC160809.03.I							x		x	X	x	X	x	X	x	X	x	X	x	X	x		x	X					x		x	X
	IC160808.12.S										X				X			x	X	x	X		X	x	X	x		x				x	X

Table 3 con't. Comparison of flash and SAM-like ramp pyrolysis.

Group	*Sample ID*	$C_{16:1}$		$C_{16:0}$		$C_{17:1}$		$C_{17:0}$		*trans*-$C_{18:2}$		*cis*-$C_{18:1}$		*trans*-$C_{18:1}$		$C_{18:0}$		$C_{19:0}$ *std*		$C_{20:0}$		$C_{21:0}$		$C_{22:0}$		$C_{23:0}$		$C_{24:0}$		$C_{25:0}$		$C_{26:0}$		$C_{27:0}$	
		F	R	F	R	F	R	F	R	F	R	F	R	F	R	F	R	F	R	F	R	F	R	F	R	F	R	F	R	F	R	F	R	F	R
Modern Active Spring System at Hveravellir	IC160730.09.S	x	X	x	X	x		x	X			x		x	X	x	X	x	X	x				x											
	IC160730.09.I			x	X			x	X							x	X	x	X	x				x											
	IC160730.01.S	x		x	X			x	X			x		x	X	x	X	x	X	x	X	x		x		x		x		x		x		x	
	IC160730.01.I	x	X	x	X			x				x		x	X	x	X	x	X	x		x		x		x		x		x		x		x	
	IC160731.08.S	x		x	X			x				x		x		x	X	x	X	x		x		x		x								x	
	IC160731.08.I1	x		x	X			x				x		x		x	X	x	X	x		x		x		x		x		x		x		x	
	IC160731.08.I2	x		x	X			x						x		x	X	x	X	x		x		x		x		x		x					
	IC160730.04.S	x	X	x	X	x		x	X	x		x		x	X	x	X	x	X	x		x		x		x		x		x		x		x	
Modern Inactive Spring System at Gunnuhver	IC160726.06.S			x	X			x	X			x				x	X		X		X		X		X		X							
	IC160726.06.I			x	X			x	X							x	X		X		X													
	IC160727.02.S			x	X			x	X							x	X		X		X		X		X		X		X					
	IC160727.02.I			x	X			x	X							x	X		X		X		X		X		X							
	IC160727.05.S	x		x	X		X	x	X		X		X	x	X	x	X		X		X		X		X		X		X		X		X	
	IC160727.05.I			x	X			x	X					x		x	X		X		X		X		X		X							
	IC160727.03.S	x		x	X		X	x	X					x	X	x	X		X		X		X		X		X		X		X		X	
	IC160727.03.I	x	X	x	X				X							x	X		X		X		X		X		X							
Relict Spring System at Lýsuhóll	IC160807.04.S	x	X	x	X			x	X		X	x		x	X	x	X	x	X	x		x		x		x		x		x		x		x	
	IC160807.04.I	x		x	X			x		x		x		x		x	X	x	X	x		x		x		x		x		x		x		x	
	IC160809.03.I	x	X	x	X	x		x	X	x		x		x		x	X	x	X	x		x		x		x		x		x		x		x	
	IC160808.12.S	x	X	x	X			x	X			x		x	X	x	X	x	X	x		x		x		x		x		x		x		x	

Table 3. Comparison of flash pyrolysis and SAM-like ramp pyrolysis of sinter samples. Green = FAME detection in both experiments.Yellow = FAME detection in flash pyrolysis experiment only. Orange = FAME detection in ramp pyrolysis experiment only. Blank cells = no FAME detection. Detection of the C_{19} standard is included for completeness.